Marine Chemistry
March 2005; 94(1-4) : 147-173
http://dx.doi.org/10.1016/j.marchem.2004.07.014

Intercalibration of benthic flux chambers II. Hydrodynamic characterization and flux comparisons of 14 different designs

A. Tengberg[a*], P.O.J. Hall[a], U. Andersson[a], B. Lindén[a], O. Styrenius[a], G. Boland[b], F. de Bovee[c], B. Carlsson[d], S. Ceradini[e], A. Devol[f], G. Duineveld[g], J.-U. Friemann[d], R.N. Glud[h], A. Khripounoff[i], J. Leather[j], P. Linke[k], L. Lund-Hansen[l], G. Rowe[m], P. Santschi[m], P. de Wilde[g] and U. Witte[n]

[a]Department of Chemistry, Marine Chemistry, Göteborg University, SE-412 96 Göteborg, Sweden
[b]Minerals Management Service, U.S. Department of the Interior, New Orleans, LA, United States
[c]Observatoire Océanologique de Banyuls, Laboratoire Arago, CNRS URA 117, F-66650 Banyuls-sur-mer, France
[d]Department of Hydraulics, Chalmers University of Technology, S-412 96 Göteborg, Sweden
[e]CISE S.p.A., Via Reggio Emilia 39, I-20090 Segrate (Mi), Italy
[f]School of Oceanography, Box 357940, University of Washington, Seattle, WA 98195-7940, USA
[g]Netherlands Institute for Sea Research, PO Box 59, 1790 AB Den Burg, Texel, The Netherlands
[h]Marine Biological Laboratory, Copenhagen University, Strandpromenaden 5, DK-3000 Helsingør, Denmark
[i]IFREMER, Centre de Brest, BP 70, F-29263 Plouzane, France
[j]Naval Command, Control and Ocean Surveillance Center, RDTE Division, 53560 Hull St., San Diego, CA 92152-5001, USA
[k]Forschungszentrum für Marine Geowissenschaften, GEOMAR, Wischhofstrasse 1-3, D-24148 Kiel, Germany
[l]Marine Ecology, Aarhus University, Finlandsgade 14, DK-8200 Århus N, Denmark
[m]Department of Oceanography, Texas A&M University, 5007 Avenue U, Galveston, TX 77551, USA
[n]Max Planck Institute for Marine Microbiology, Celsiusstrasse 1, D-28359 Bremen, Germany

*: Corresponding author : Tel.: +46 31 772 2776; fax: +46 31 772 2785. anderste@chem.gu.se

Abstract: We have compared 14 different sediment incubation chambers, most of them were used on bottom landers. Measurements of mixing time, pressure gradients at the bottom and Diffusive Boundary Layer thickness (DBL) were used to describe the hydrodynamic properties of the chambers and sediment–water solute fluxes of silicate (34 replicates) and oxygen (23 replicates) during three subsequently repeated incubation experiments on a homogenized, macrofauna-free sediment. The silicate fluxes ranged from 0.24 to 1.01 mmol m−2 day−1 and the oxygen fluxes from 9.3 to 22.6 mmol m−2 day−1. There was no statistically significant correlation between measured fluxes and the chamber design or between measured fluxes and hydrodynamic settings suggesting that type of chamber was not important in these flux measurements. For verification of sediment homogeneity, 61 samples of meiofauna were taken and identified to major taxa. In addition, 13 sediment cores were collected, sectioned into 5–10-mm slices and separated into pore water and solid phase. The pore water profiles of dissolved silicate were used to calculate diffusive fluxes of silicate. These fluxes ranged from 0.63 to 0.87 mmol m−2 day−1. All of the collected sediment parameters indicated that the sediment homogenization process had been satisfactorily accomplished. Hydrodynamic variations inside and between chambers are a reflection of the chamber design and the stirring device. In general, pump stirrers with diffusers give a more even distribution of bottom currents and DBL thicknesses than paddle wheel-type stirrers. Most chambers display no or low static differential pressures when the water is mixed at rates of normal use. Consequently, there is a low risk of creating stirrer induced pressure effects on the measured fluxes. Centrally placed stirrers are preferable to off-center placed stirrers which are more difficult to map and do not seem to give any hydrodynamic advantages. A vertically rotating stirrer gives about five times lower static differential pressures at the same stirring speed as the same stirrer mounted horizontally. If the aim is to simulate or mimic resuspension at high flow velocities, it cannot be satisfactorily done in a chamber using a horizontal (standing) rotating impeller (as is the case for most chambers in use) due to the creation of unnatural conditions, i.e. large static differential pressures and pre-mature resuspension at certain locations in the chamber.

Keywords: Benthic chambers; Calibration; Hydrodynamic properties; Comparative flux incubations

Intercalibration of benthic flux chambers II. Hydrodynamic characterization and flux comparisons of 14 different designs

A. Tengberg[1*], P. Hall[1], U. Andersson[1], B. Lindén[1], O. Styrenius[1], G. Boland[2], F. de Bovee[3], B. Carlsson[4], S. Ceradini[5], A. Devol[6], G. Duineveld[7], J-U. Friemann[4], R.N. Glud[8], A. Khripounoff[9], J. Leather[10], P. Linke[11], L. Lund-Hansen[12], G. Rowe[13], P. Santschi[13], P. de Wilde[7] and U. Witte[14]

[1]*Dept. Chemistry, Göteborg University, SE-412 96 Göteborg, Sweden*

[2]*Minerals Management Service, U.S. Department of the Interior, New Orleans, Louisiana.*

[3]*Observatoire Océanologique de Banyuls, Laboratoire Arago, CNRS URA 117, F-66650 Banyuls-sur-mer, France*

[4]*Dept. of Hydraulics, Chalmers Univ. of Technology, S-412 96 Göteborg, Sweden*

[5]*CISE S.p.A., Via Reggio Emilia 39, I-20090 Segrate (Mi), Italy*

[6]*School of Oceanography, Box 357940, University of Washington, Seattle, WA 98195-7940, USA*

[7]*Netherlands Institute for Sea Research, PO Box 59, 1790 AB Den Burg, Texel, The Netherlands*

[8]*Marine Biological Laboratory, Copenhagen University, Strandpromenaden 5, DK-3000 Helsingør, Denmark*

[9]*IFREMER, Centre de Brest, BP 70, F-29263 Plouzane, France*

[10]*Naval Command, Control & Ocean Surveillance Center, RDTE Division, 53560 Hull St., San Diego, CA 92152-5001, USA*

[11] *Forschungszentrum für Marine Geowissenschaften, GEOMAR, Wischhofstrasse 1-3, D-24148 Kiel, Germany*

[12]*Marine Ecology, Aarhus University, Finlandsgade 14, DK-8200 Århus N, Denmark*

[13]*Dept. of Oceanography, Texas A&M University, 5007 Avenue U, Galveston, TX 77551, USA*

[14] *Max Planck Institute for Marine Microbiology, Celsiusstrasse 1, D-28359 Bremen, Germany*

*Corresponding author E-mail address: atengberg@zi.ku.dk

Keywords: Benthic chambers, Calibration, Hydrodynamic properties, Comparative flux incubations

---

Abstract

We have compared fourteen different sediment incubation chambers, most of them used on bottom landers. Measurements of mixing time, pressure gradients at the bottom and Diffusive Boundary Layer thickness (DBL) were used to describe the hydrodynamic properties of the chambers and sediment-water solute fluxes of silicate (34 replicates) and oxygen (23 replicates) during three subsequently repeated incubation experiments on a homogenized, macrofauna free sediment. The silicate fluxes ranged from 0.24 to 1.01 mmol m^{-2} day^{-1} and the oxygen fluxes from 9.3 to 22.6 mmol m^{-2} day^{-1}. There was no statistically significant correlation between measured fluxes and the chamber design or between measured fluxes and hydrodynamic settings suggesting that type of chamber was not important in these flux measurements. For verification of sediment homogeneity 61 samples of meiofauna were taken and identified to major taxa. In addition 13 sediment cores were collected, sectioned into 5-10 mm slices and separated into pore water and solid phase. The pore water profiles of dissolved silicate were used to calculate diffusive fluxes of silicate. These fluxes ranged from 0.63 to 0.87 mmol m^{-2} day^{-1}. All of the collected sediment parameters indicated that the sediment homogenization process had been satisfactorily accomplished. Hydrodynamic variations inside and between chambers are a reflection of the chamber design and the stirring device. In general, pump stirrers with diffusers give a more even distribution of bottom currents and DBL thicknesses than paddle wheel type stirrers. Most chambers display no or low static differential pressures when the water is mixed at

rates of normal use. Consequently there is a low risk of creating stirrer induced pressure effects on the measured fluxes. Centrally placed stirrers are preferable to off-center placed stirrers which are more difficult to map and do not seem to give any hydrodynamic advantages. A vertically rotating stirrer gives about 5 times lower static differential pressures at the same stirring speed as the same stirrer mounted horizontally. If the aim is to simulate or mimic resuspension at high flow velocities it cannot be satisfactory done in a chamber using a horizontal (standing) rotating impeller (as is the case for most chambers in use) due to the creation of unnatural conditions, i.e. large static differential pressures and pre-mature resuspension at certain locations in the chamber.

1. Introduction

Even though almost 60 % of the surface of the earth consists of deep-sea abyssal plains, our biogeochemical knowledge about these huge areas of our planet is limited. Coring and recovery of the deep-sea bottom is often accompanied by physical changes (in pressure, temperature, light, etc.), which make it difficult to obtain representative samples and data. Artifacts in chemical and biological activity associated with sample recovery can occur already at shallow depths (e.g. Koop et al., 1990), but they escalate in the deep sea (e.g. Murray et al., 1980; Berelson et al., 1990; Glud et al., 1994; Aller et al., 1998). For this reason, and in spite of technical difficulties, many investigations have been performed directly on the sea floor using benthic *in situ* landers (for reviews, see Berelson et al., 1987; Tengberg et al., 1995).

One type of benthic lander, the so called chamber landers, carry flux chambers which are designed to isolate a limited area of the sea-floor together with the overlying water. Benthic exchange rates are then calculated from concentration change of the relevant

solutes in the enclosed water - either by direct measurements with sensors or discrete water sampling and later analysis.

To assure mixing, so that the measured concentration changes in the incubated water are representative for the enclosed sediment and volume of overlying water, and sometimes to maintain hydrodynamic conditions as close as possible to those existing outside the chamber, all chambers are equipped with water mixing mechanisms (e.g. paddle wheels, pumps, magnetic stirring bars, etc.). Chambers vary considerably both in shape, size and the mixing device leading to varying hydrodynamic conditions. The water movement inside the chamber is also dependent on the location of the stirring mechanism (Buchholtz-Ten Brink et al., 1989; Shaw, 1994) and/or if hydrodynamic obstacles (e.g. sensors or sampling systems) are present. It is critical to know if the specific hydrodynamic conditions associated with a specific chamber design result in biased flux measurements (e.g. Berelson et al., 1986).

Some commonly used parameters to characterize hydrodynamic conditions are boundary layers (both logarithmic and diffusive), pressure gradients and shear stress. In the oceans, boundary layers are normally turbulent with logarithmically decreasing velocity profiles when approaching the bottom (e.g. Hinze, 1975; Gust and Weatherly, 1985). In the lowest part of the boundary layer, the so called diffusive boundary layer (DBL), the water movements are too low to cause any advective vertical transport of solutes. Here solute transport is controlled by molecular diffusion. The DBL thickness is solute dependent and regulated by water flow velocity, bottom roughness and viscosity. The DBL may impede solute exchange between sediment and the water (e.g. Boudreau and Guinasso, 1982; Jørgensen, 1983a), an effect commonly observed when oxygen consumption is high or bottom water concentrations are low (e.g. Jørgensen and Revsbech, 1985; Hall et al., 1989; Jørgensen and Des Marais, 1990).

Estimates of chamber hydrodynamics and direct *in situ* measurements of diffusive boundary layer thicknesses have previously been made either with pressure gauges and (oxygen) microelectrodes (Glud et al., 1995), skin friction probes (Gust, 1988), by alabaster or hydrohinone dissolution (Santschi et al., 1983; Opdyke et al., 1987; Buchholtz-Ten Brink et al., 1989; Berelson et al., 1990; Santschi et al., 1991; Vershinin et al., 1994) or by radiotracer uptake by the seabed (Santschi et al., 1984; Hall et al., 1989; Sayles and Dickinson, 1991; Dickinson and Sayles, 1992).

Three different designs of benthic chambers were recently described hydrodynamically and replicate flux measurements were made on homogenized, macrofauna-free sediment (Tengberg et al., 2004). It was found that hydrodynamics, within the ranges of applied shear stress, DBL thickness and total pressure, did not have any significant influence on the measured fluxes in the coastal, cohesive sediment used. A comparison of fluxes measured in the chambers with those calculated from pore water gradients illustrated that the three chamber types all measure benthic fluxes accurately. In this companion paper we extend our comparisons of mixing time, pressure gradients, DBL thickness, and benthic silicate and oxygen fluxes to 14 designs of chambers, most of which are used *in-situ* on landers. A comparative study of so many existing chamber designs has not, to our knowledge, been made previously.

The aims of this paper are:

* To characterize hydrodynamically each of the participating chambers with regard to flow pattern, mixing time, pressure gradients and DBL.

* To make a direct comparison of fluxes measured by the participating chambers in a homogenized sediment.

* To evaluate statistically to which extent any differences in fluxes obtained by the various chambers is related to differences in hydrodynamics and/or chamber design.

2. Materials and Methods

2.1. Participating chamber designs

The intercalibration involved 14 different designs of chambers that isolate sediment surface areas between 78 cm^2 and 12,100 cm^2. Fig. 1 summarizes information about the different chamber designs, their normal application and the measurements conducted with them in the present work. The LINKE chamber was much larger than the rest. The design was chosen to enclose a large sediment area above seeps, to focus the outflow towards a flow meter mounted on top of the chamber and to reduce the enclosed water volume for a more rapid mixing of the dissolved vent constituents. This chamber differs both in use and design, compared to the rest, and has thus been treated separately in the following.

The water mixing devices varied from paddle wheels to pumps with diffusers. In the following we refer to rotating objects (paddle wheels, bars or plates) by the word “stirrer”. For several of the measurements (e.g. visualization) and for practical reasons, transparent - but otherwise identical - copies (mainly in Plexiglas) of each chamber was used. These were equipped with their normal water mixing devices and "hydrodynamic obstacles" (water sampling systems, electrodes etc.). For all experiments, except the flux incubations (see below), a transparent dummy bottom was fixed to the chamber in order to mimic the sea floor and to ensure that the water height corresponded to that normally applied in the chamber. The dummy bottom has a smoother roughness than natural sediments and therefore some differences should be expected between the results obtained here and natural conditions, which are more variable. These experiments should still give indications on the differences and similarities in hydrodynamic properties that exist between the chambers. The intercalibration took three weeks and was organized into four different sections (called workstations below).

2.2. Workstation I: Visualization and mixing time experiments

A visualization experiment was carried out and video-filmed to get a first rough estimate of the movement (vortices, stagnant zones, etc.) in each chamber. A two dimensional picture of the three-dimensional flow field was created by mixing light reflecting aluminum particles in the water and illuminating them with a strong lamp (500 W) through a 10 mm wide slit. The aluminum particles were small (average size 40 μm) and stayed in suspension for several hours after the mixing was stopped.

Estimates of the mixing time in the chambers were made by keeping the pH of the chamber water at the transition point for the indicator phenolphthalein, alternately injecting base and acid in equivalent molar amounts and following the corresponding color changes. The additions were made at the chamber lid by directing a base/acid filled automatic pipette towards the bottom and injecting promptly, thereby the heavy indicator fluid sank to the bottom from where it was mixed upwards in the chamber. It is important during chamber incubations that the concentrations of solutes in the upper part of the chamber are identical to those close to the bottom, since sampling of water and electrode measurements during incubations typically are made close to the lid. The time for complete mixing, of the base/acid being mixed from the bottom, was estimated visually with a stop watch.

2.3. Workstation II: Measurements of differential pressures

Previous measurements of pressure differences in chambers have been carried out with commercially available gauges (Huettel and Gust, 1992a; Huettel and Gust, 1992b; Glud et al., 1995). In this study, a special setting of ten pressure gauges was developed because commercial gauges are sensitive to over-pressures, expensive and only measure at one "channel" at a time.

For calibration the chamber, undergoing evaluation, was filled to the top with water and was left open. By gently adding or retrieving water at the top with an automatic pipette

(±0.01 ml precision) different pressure gradients were imposed simultaneously on the ten measuring cells. Each pressure sensor had a resolution of ±0.03 Pa and was linear in a range between 0-200 Pa (1 Pa = 0.1 mm water column), however the response was individual and consequently the calibration was performed individually for each pressure sensor. Calibrations were made before and after evaluating each chamber to keep control over drift or hysteresis phenomena. For more detailed information about this equipment see Tengberg et al. (2004).

The aim of the measurements was to locate areas with extreme pressure gradients, when the chambers were mixed at the most frequently applied speed/flow. A measurement strategy for each chamber was individually selected after studying the video recording from the mixing experiments (see section 2.2. above). Transect(s) of holes (7 to 69 depending on chamber symmetry and size, Fig. 1) were carefully drilled, smoothed and equipped with adapters on the lower side of the Plexiglas dummy bottom. Ten five-minute measuring cycles, with the stirrer/pump on during 2.5 minutes and off during 2.5 minutes, were the normal procedure for each chamber.

Experiments were performed in some of the chambers by placing stainless steel nets of different mesh sizes (100, 150, 200 μm) on the chamber bottom to test potential effects of bottom roughness on the differential pressures. No significant effects were observed and consequently no nets were used when evaluating the chambers.

2.4. Workstation III: Alabaster plate dissolution to estimate the diffusive boundary layer thickness

The thickness of the DBL is often estimated from the dissolution rate of solid materials e.g. alabaster or hydrohinone (Santschi et al., 1983; Opdyke et al., 1987; Buchholtz-Ten Brink et al., 1989; Berelson et al., 1990; Santschi et al., 1991; Vershinin et al., 1994). The dissolution rate is typically quantified from the weight loss during an

experiment. From the molecular diffusion coefficient of the dissolved material and the potential saturation concentration, an estimate of the boundary layer thickness (Z in μm) can be calculated from eq. 1:

$$Z = \frac{D_{Ca^{2+}} * [Ca^{2+}]_{sat}}{F} \quad (1)$$

in which F is the flux:

$$F = \frac{(\text{alabaster plate weight loss [g]}) * 0.2328}{(\text{surface area of alabaster plate [cm}^2\text{]}) * (\text{time exposed to dissolution [sec]})} \quad (2)$$

D_{Ca2+} = molecular diffusion coefficient for Ca^{2+} at the given temperature [10^{-5} cm^2 s^{-1}].
$[Ca^{2+}]_{sat}$ = Ca^{2+} concentration at alabaster saturation for the given temperature [g cm^{-3}].
The constant 0.2328 used in eq. 2 is the relative Ca^{2+} content in each alabaster plate.

Applying eq. 1 assumes a linear dissolved Ca^{2+} increase in the overlying water which was tested in each of our chamber experiments.

For this study, approximately 4 x 4 cm^2, 5 mm thick alabaster plates were used (cut from sculpture alabaster, Sculpture House, New York City, NY, USA). The number of plates (between 3 and 5) varied with the size of each chamber (Fig. 1). The bottom and all sides of each plate were painted with polyurethane to prevent dissolution from non-directly exposed surfaces. The plates were measured and weighed before placing them into specially cut depressions in PVC bottoms constructed for each experimental chamber. After placement of the plates, the chambers were filled with a known volume of distilled water (with a measured Ca^{2+} concentration of 1.6 μM), the lid was attached, all air was removed (through two valves) and the stirring device started.

Participating chambers were incubated for 14 hours at constant temperature (19.0 ± 1° C). Six samples (30 ml each) were taken from the overlying water of each chamber and analyzed for dissolved Ca^{2+} using an atomic absorption spectrophotometer (Perkin Elmer model #3110, analytical precision about 0.5% RSD). Replacement water with an average Ca^{2+}-concentration of 1.6 µM was added.

After the experiment, the plates were carefully removed from the embedding material and allowed to dry at room temperature until no additional weight loss between repeated weighing was observed. Equation (1) was used to calculate diffusive boundary layer thicknesses for individual plates and for all plates combined in each chamber. Values of $[Ca^{2+}]_{sat}$ and D_{Ca2+} were temperature corrected after Christoffersen and Christoffersen (1976) and Buchholtz-Ten Brink et al. (1989). Corrected values for D_{Ca2+} were obtained by entering viscosity values (v) at the appropriate temperature and using the relation $D_1/D_2 = v_2/v_1$ (Poisson and Papaud, 1983).

2.5. Workstation IV: Comparative flux-incubations

A direct comparison of measured fluxes was carried out by incubating the chambers simultaneously under controlled laboratory conditions in the same homogenized sediment. Concentration change of solutes in the overlying water as a function of time was used as a direct measure of solute fluxes across the sediment-water interface.

With an anchor dredge, two cubic meters of a silty sediment were collected at 34 m water depth (SE of Lilleskär in the Koster Fjord, western Sweden) and sieved through 5 mm mesh. The sediment was then mixed with 200 l of "industrial" sand and 400 l of bottom water (from the sampling site) in a 6 cubic meter truck mixer. Consequently this sediment contained a volume ratio of 10:1:2 (sediment:sand:water). After three hours of mixing, the homogenized sediment was carefully poured into two rectangular tanks placed in a dark

thermo-constant room (8.3 ± 0.3° C). The size of the tanks was 2 m x 3 m, and the sediment was filled to an average sediment depth of 17 cm. On top of the sediment, 30 cm of seawater (bottom water from the sampling site) was gently added. The tanks were left for 20 days with constant air bubbling, which also created a gentle mixing of the overlying water. After this time the tank-water concentration of dissolved silicate had increased from 8.9 µM to 40.6 µM. In order to maintain a significant concentration difference (and consequently a high efflux) between the overlying water and the sediment pore water, the overlying water in tank 1 was exchanged with fresh bottom water from the sampling site 8.5 days before the chamber incubations were initiated there. The water in tank 2 was exchanged 3.5 days before the incubations started in this tank.

To compare flux results from the different chambers, the sediment must be homogenous. Eleven replicate incubations (three in tank 1 and eight in tank 2) with the GÖTEBORG 1 chamber were performed in order to quantify any potential heterogeneous distribution of the benthic exchange rates in the two tanks. Additionally pore water profiles of silicate were measured on retrieved cores. 13 cores of 6.2 cm^2 (7 in tank 1 and 6 in tank 2) were taken by gently inserting 50 ml syringes from which the edge had been cut off. These cores were taken after the incubations were finished but before the chambers were retrieved from the tanks. The sediment was sectioned into 4 mm slices in the top and coarser intervals (5-10 mm) below, and put into centrifuge tubes. The pore water and the solid phase were separated by centrifugation for 30 minutes at 2100 RPM. While the pore water was filtered (0.45 µm pore size cellulose acetate filters) and analyzed for dissolved silicate concentrations (spectrophotometrically according to Strickland and Parsons, 1968), the solid phase from all surface samples and two full depth profiles were analyzed for the content of total carbon, organic carbon and total nitrogen (using a Carlo Erba CHN analyzer mod. NA1500NC). From the pore water profiles of silicate, effluxes were calculated using the methods described in Berg et al. (1998). Since the sediment type and temperature for the

flux incubations were almost identical in the previous and the present intercalibration study, the procedures, diffusion coefficients and porosities used to calculate silicate fluxes from the pore water profiles were adopted from Tengberg et al. (2004).

Furthermore, sampling for metazoan meiofauna (31 samples in tank 1 and 30 in tank 2) was carried out with 3.8 cm^2 tubes to a depth of 5 cm both in the sediment incubated by the chambers and outside the chambers (for the exact location of the different samples, see Fig. 2 and Fig. 3). These samples were gently washed with tap water through a 40 µm sieve. The animals retained on the sieve were extracted from the sediment by centrifugation in Ludox HS-40 (McIntyre and Warwick, 1984). Organisms were identified to the major taxa (nematodes, copepods, kinorynchs, ostracods, bivalves, annelids, ophiures and arcariens) and counted under a stereoscopic microscope.

Flux incubations were started by gently inserting all the participating chambers into the sediment of the same tank and closing their lids (see Fig. 2 and Fig. 3 for emplacement of the chambers in the tanks). Each lid was equipped with two valves; one for collection of water samples and the other for entry of replacement water from the tank. To ensure that the chambers maintained the same sediment penetration depth throughout the incubation they were either equipped with fringes or pushed so that their edges, or (for some chambers) mounted "stilts", stood on the tank bottom. In all cases, the aim was to use the same height of overlying water which was typical for normal applications. For an accurate estimate of the incubated water volume a known amount of Br^- was injected into each chamber. This amount varied as a function of the nominal chamber volume with the intention of reaching an approximate Br^- concentration of 7 mM after the chamber water had been fully mixed. From the mixing time experiment (see 2.2. above) an estimate of the time needed for complete mixing was obtained (t_{mix}). The first sample of the chamber water was taken 2 * t_{mix} after the injection. The use of Br^- dilution for chamber volume determination has been practised by lander operators previously (e.g. Jahnke and Christiansen, 1989; Sayles and

Dickinson, 1991; Martin and Banta, 1992; Dickinson and Sayles, 1992; Glud et al., 1995; Sayles and Martin, 1995), and it also gives the possibility to check if a chamber is leaking.

A total of three subsequent 60 hour chamber incubations (one in tank 1 and two in tank 2) including all chamber designs were carried out. Throughout each of the incubations, 7-8 samples were taken at regular time intervals from the overlying water in each chamber. At each sampling occasion, one 50 ml glass syringe was used to sample for oxygen, and one 50 ml polypropylene syringe for silicate and bromide. Prior to analysis (silicate) or storage (bromide), the samples in the plastic syringes were filtered through cellulose acetate filters (0.45 μm pore size). All filters were rinsed with 100 ml of Milli-Q water prior to use. Determinations of silicate (Strickland and Parsons, 1968) and oxygen (by Winkler titration with a precision of around 0.6 %) were made immediately after each sampling occasion. Samples were stored in a refrigerator and analyzed for bromide two weeks after the intercalibration workshop by ion chromatography (Dionex mod. 4500i; precision better than 1 %).

The known volume of replacement water, which entered the chambers from the tank at each sampling occasion, was regularly analyzed for Br^-, O_2 and Si. When calculating the fluxes in each chamber, compensations were made for the replacement water. Moreover, the Biological Oxygen Demand (BOD) of the tank water was measured throughout all incubations by regularly incubating tank water samples in Winkler bottles. The oxygen consumption measured in the water of each chamber was corrected for the corresponding BOD. Hence, all oxygen fluxes reported in this paper solely represent sediment oxygen uptake rates.

2.6. Statistical data evaluation

For statistical evaluation the results from this study were divided into two groups that were evaluated separately. The first evaluation was made to quantify the degree of smaller and larger scale sediment heterogeneity, both within and between tanks. Calculated dissolved silicate fluxes, from the collected pore water profiles, and meiofauna samples were compared using both one-and two way analysis of variance (ANOVA) with Student Newman Keuls multiple comparisons *a posteriori* (Underwood, 1997). First the individual sampling spots were compared with each other. Then a two way ANOVA, a nested design, was used and homogeneity of variance was tested with a Cochran C test (Snedecor and Cochran, 1967). For meiofauna, four replicates were chosen randomly in each "meiofauna chamber" (see Fig. 2 and 3) and four replicates from the tank sediment outside the chambers. Each four-replicate spot was regarded as a locality, giving a total of six such spots in each tank. In the same way three localities with two silicate profiles (and the corresponding calculated effluxes) were chosen in each tank and compared.

The second statistical data treatment was done to asses if statistically significant differences occurred between the chamber measured fluxes (of silica and oxygen) and if so which factors (tank number, chamber type, chamber shape (cylindrical or squared), chamber incubated water volume, mixing time, exposed sediment area, chamber water height, average DBL, worst case differential pressure and meiofauna in the chamber) were causing such differences to occur. To analyze relationships between variables, simple linear regression was used to test if there was a statistically significant relationship and how large the explained variance (R^2) was.

In all cases the software Statistica 6.0 (from Statsoft Inc) was used and a significance level of P=0.05 was maintained.

3. Results and Discussion

3.1. Workstation I: Visualization and mixing

For chambers with rotating stirrers the main motion patterns could be divided into three general parts: rotation around the main vortex axis; two separated water circulation areas, above and below the impeller; the water left the impeller tip directed outwards and against the chamber wall and was sucked into the impeller through the main vortex (Fig. 4a). These basic patterns were present in all stirred chambers. Geometric obstacles only modified the basic water movement pattern. The flow in eccentrically stirred chambers also contained a main vortex, but positioned diagonally through the chamber (Fig. 4b).

In chambers with pumps the water left the outlet like a water jet. The jet was directed straight forward and only deflected at physical obstacles. In the DE WILDE chamber, there was one large outflow (Fig. 1), that created a stream following the chamber wall towards the inflow, creating a more or less stagnant zone in the middle (Fig. 4c). This can be compared with the ROWE chamber with many outflows to the bulk volume, which resulted in a more homogeneous flow giving a more uniform distribution of velocities, DBL thicknesses and (by analogy) shear stresses.

It is important to remember that for the mixing times there were no exact results (Table 1). Unavoidable small variability in the acid/base addition procedure resulted in some differences in the obtained mixing time. It is furthermore difficult to decide exactly when the entire volume of chamber water had changed color. However, in chambers with long mixing times (10 minutes or more), there may be development of thick diffusive boundary layers over large areas above the sediment surface, and if the sampling is frequent the samples may not represent the average conditions in the chamber.

It is worth noting that no difference in mixing time could be noticed for the CISE chamber when increasing the number of stirring bars from 1 to 4 on the impeller (Fig. 1). However, addition of bars led to the creation of higher differential pressures (Table 1). The

most probable explanation is that the addition of bars led to a more stable circulation pattern which created a higher static pressure.

Mixing time experiments can give valuable information on the main type of water flow (turbulent, transient or laminar) in a chamber (Edwards, 1985). By doing several mixing time experiments at different mixing rates and by plotting the mixing times against the stirring speeds/pump flows, a distinct prolongation in the mixing times could be noticed, with only minor decreases in the stirring speed/pump flow, when passing from a mainly turbulent to a laminar flow regime in the chamber. Taking the GÖTEBORG 1 chamber as an example we observe that when stirring rates are decreased below 10 RPM the mixing time increases considerably faster than above 10 RPM. This indicates that at about 10 RPM the chamber mixing is in the transition between turbulent and laminar flow. (Fig. 5).

The visualization and pressure experiments were made in the laboratory at a temperature of approximately 19°C using fresh water. When measuring *in situ*, salinity, temperature and hydrostatic pressure are often different, normally resulting in a higher water viscosity which leads to slightly longer mixing times and lower maximal pressure gradients than were measured here.

3.2. Workstation II: Pressure

The maximal differential pressures for the participating chambers are presented in Table 1. For chambers with a stirrer placed in the center the maximal pressure differences, if any was detected, occurred between the center, where the pressure is negative due to the rising water flow in the vortex, and the periphery, where the pressure is slightly positive (see Fig. 6 for and example from the CISE chamber). For most chambers the maximal current speeds were low (0-2.5 cm s^{-1}, data not shown) and no (< 0.3 Pa) differential pressures could be detected. Detectable differential pressures were measured in six chambers; GÖTEBORG 1, GÖTEBORG 2, ROWE, AARHUS, WITTE and CISE. In the

CISE chamber the maximal differential pressure increased from 1.3 Pa to 3.4 Pa when the number of stirring bars was increased from 2 to 4 (Table 1). Maximal current speed in the chamber was approximately 3.5 cm s^{-1} at this occasion.

When increasing the stirring rate (from 21 to 40 RPM) in the off-center stirred GÖTEBORG 1 chamber the vortex center, and thereby the spot with minimal pressure, moved. The same phenomenon took place in the GÖTEBORG 2 chamber with changing stirring rates. At 40 RPM the maximal current speed in the GÖTEBORG 1 chamber was around 5 cm s^{-1} (data not shown) and the maximal differential pressure was 9.6 Pa. The same stirring speed (40 RPM) in the GÖTEBORG 2 chamber gave roughly the same maximal current speed, but with a more evenly distributed velocity pattern (Lund-Hansen et al., unpublished results) and a considerably lower maximal differential pressure of 2.0 Pa. This implies that a vertical stirring device is better in avoiding static differential pressures than a horizontal stirrer. These findings are further confirmed in Tengberg et al. (2004). Prior to the intercalibration the asymmetrical GÖTEBORG 1 chamber was compared with the same chamber in which the stirrer was placed in the center. No significant difference in pressure was found between these two designs leading to the conclusion that there are no advantages, regarding pressure, and probably not regarding other hydrodynamic aspects as well, with a stirrer that is placed off center. On the contrary, the hydrodynamics in a chamber with a centrally placed stirrer is easier to map and to understand, and therefore probably preferable.

For the ROWE chamber a negative pressure of 2.2 Pa developed due to the proximity of one of the pump inlets to the bottom. Most of this pressure (1.5 Pa) disappeared when this pump was stopped (Table 1). If moving the inlet to a higher position above the bottom or directing it differently the pressure effect would probably decrease.

When comparing pressures in chambers it is important to remember that the driving force is the pressure gradient at the sediment surface, approximated by the ratio between the

differential pressure and over what distance it acts. Depending on the permeability of the sediment, a higher differential pressure in a big chamber (such as CISE) is of less importance for the possible creation of artifacts than the same (or lower) differential pressure in a smaller chamber.

Since the small AARHUS chamber has mainly been employed to do resuspension studies in a laboratory (Lund-Hansen et al., 1999), it was tested at relatively high stirring rates. A differential pressure of 7.5 Pa was developed at 34 RPM, but at this rate the maximal current speed in the chamber close to the bottom was considerably higher (9.1 cm s^{-1}) than in the other chambers. This current speed has in previous studies been the lower limit to cause resuspension of coastal organic rich (around 11 % by weight) silty clays (Lund-Hansen et al., 2002). If the aim is to simulate or mimic at what shear velocity (u*) resuspension is created, chambers with horizontal (standing) rotating impeller are most likely less suitable due to an uneven and chaotic shear velocity and DBL distribution at the bottom. The data in this study gave similar indications, as did the studies by Gust and Müller (1997) and Tengberg et al. (2004). In these two studies the so called Microcosm design (Gust, 1990) was found to be the most suitable instrument to create an even distribution of shear stress and diffusive boundary layer thickness at both low and high current speeds. However, the latter study also demonstrated that the Microcosm develops higher pressure gradients than several other chambers, at similar shear velocities.

In permeable sediments static pressure differences at the bottom of a benthic chamber during incubations can give rise to artificial exchanges between the sediment and the overlying water. With the same shear stress up to 6 times higher solute release rates were found in a stirred cylindrical chamber containing a fine sandy sediment, compared with the release rate in a flume outside. This was shown to be caused by advective flow (pumping) in the sediment generated by stirring induced static pressure differences (of around 3 Pa) at the sediment surface in the chamber (Huettel and Gust, 1992a). The critical

sediment permeability limits for the creation of pumping artifacts, giving enhanced fluxes, have been evaluated with the help of conservative tracers such as Rhodamine-WT dye (Huettel and Gust, 1992a) and Br^- (Glud et al., 1996). In the latter study it was concluded that data obtained by benthic chambers in sediments with a permeability exceeding $2*10^{-12}$ m^2 (sandy sediments) have to be evaluated with care if the water mixing device in the chamber creates differential static pressures of 2-3 Pa. By lowering the stirring rate the differential pressures decreased, resulting in an increase in the critical permeability, by at least 1 order of magnitude (Glud et al., 1996). During normal use the only chambers in this study that could suffer from potential stirrer induced pressure effects when being used on permeable sediments were the ROWE and CISE chambers. These artifacts can easily be avoided by using only one stirring bar in the CISE chamber and by moving the location of the pump further up in the ROWE chamber (see above).

Previous studies, in relatively shallow environments, have indicated the importance of changing current speeds and directions (and consequently changing differential pressures, DBL thicknesses, etc.) for sediment infaunal short-term (within hours) and long-term (within days and weeks) activity and growth (Vogel, 1981; Jørgensen, 1983b; Lenihan et al., 1996). Furthermore, it is well known that faunal activity can enhance sediment-water exchange rates both by increasing the actual permeability through construction of burrows and channels, and by bioirrigation (e.g. Aller, 1982; Rutgers van der Loeff et al., 1984; Huettel and Gust 1992b; Aller and Aller, 1992). This implies that even if fluxes are not limited by DBL thickness or not influenced by differential pressure per se, it may be of importance to simulate *in situ* hydrodynamical conditions in chambers because of the benthic faunal response to changes in hydrodynamics.

3.3. Workstation III: Diffusive boundary layer thickness

DBL thicknesses in this study were obtained from dissolution of alabaster plates. Individual plate DBL thickness values (Z) ranged from 230 to 1029 μm (Table 1). Average DBL thickness ranged from 294 μm for the CISE chamber to 711 μm for the IFREMER chamber. The calcium increase rate in the overlying water was constant in all chambers (r^2 varied from 0.966 to 0.998; Fig. 7).

All chambers exhibited variations of mass loss between individual plates resulting in a spatial variation of estimated boundary layer thicknesses. It is worth noting that in the asymmetrically stirred IFREMER chamber, which had an average DBL thickness of 711 μm, the two plates (A2 and A25, Fig. 1) which were placed on the greatest distance from the stirrer also showed the thickest DBL of 963 and 767 μm, respectively. As discussed previously (section 3.1.) the vortex rises diagonally in eccentrically stirred chambers which would explain why the DBL for the plate placed under the stirrer (A22) was not relatively thicker (595 μm). The IFREMER chamber is equipped with three water sample bottles inside the chamber (Fig. 1). These constitute hydrodynamic obstacles which change the circulation pattern and slow down the current speeds probably giving rise to thicker DBL at the plates A2 and A25.

In the BMIC chamber, plate A19 placed directly under the vertically rotating magnet gave the thinnest DBL (255 μm), and in the CISE chamber the thickest (322 μm) occurred in the center and the thinnest (254 μm) close to the chamber wall. This last feature is a logical consequence of the uprising current in the middle and has been observed previously (e.g. Glud et al., 1995). The WITTE, GÖTEBORG 1 and NAVAL COMMAND chambers indicated similar average boundary layer thicknesses of 474, 486 and 401 μm, respectively, with relatively small variations within each chamber of 12-18 % (calculated as standard deviation/mean). In the DE WILDE chamber, for which two experimental runs were made, plates placed at the same position during each of the runs gave similar results (Table 1). One emplacement (D5/D15, Fig. 1) exposed a significantly thinner DBL during both the

experiments (253 and 230 μm compared to averages of 426 and 413 μm). The DBL variation in this chamber is probably caused by the water jet of the chamber. This feature was also observed during the visualization (see section 3.1.).

In situ benthic diffusive boundary layer (DBL) thicknesses have previously been measured with the use of oxygen μ-electrodes (Archer et al., 1989; Gundersen and Jørgensen, 1990; Glud et al., 1994), with hydrohinone (Vershinin et al., 1994) and alabaster plates (Santschi et al., 1991). The latter authors observed a DBL thickness of 500-1200 μm (with varying flow velocities of 2-8 cm s^{-1} measured at a height above the bottom of 100 cm). Inside chambers direct measurements of DBL thicknesses have been made both with μ-electrodes, alabaster plates, radiotracer uptake and hydrohinone (Devol, 1987; Buchholtz-Ten Brink et al., 1989; Hall et al., 1989; Sayles and Dickinson, 1991; Dickinson and Sayles, 1992; Glud et al., 1995). Jørgensen and Des Marais (1990) showed that on a microbial mat the DBL was limiting the oxygen flux and when decreasing the DBL thickness from 590 to 160 μm the oxygen uptake rates increased from 56 to 135 mmol m^{-2} day^{-1}. In the study presented in Tengberg et al. (2004), which was made at almost identical conditions as the work presented here, the average chamber DBL was varied from approximately 120 to 550 μm without any noticeable influence on the measured oxygen and nutrient fluxes. Thus, the chamber-averaged DBL thickness was apparently not a limiting factor on that sediment which had oxygen fluxes of about 11 mmol O_2 m^{-2} day^{-1}, which is a typical magnitude for many coastal and shelf sediments.

For the chambers described here the average DBL varied from 294 to 711 μm. These are values that can often be encountered in the natural environment, especially when working in areas which are unaffected by wave action. In this study the DBL thickness did not have any significant influence on the measured fluxes of oxygen and silica and consequently, with respect to DBL thickness, the choice of chamber did not affect the measured flux rates.

3.4. Workstation IV: Flux comparisons

The counting of thirty-one meiofauna samples in tank 1 showed an average of 412±70 (17 % variation, SD/mean) individuals. The number was similar in tank 2, 380±73 (19 %, for 30 samples). Nematodes were the largely dominating taxon and although all the other meiofaunal taxa were occasionally found their total amount never exceeded 8 individuals in any of the 61 samples. A two factor ANOVA (to compare tank 1with tank 2) and two one factor ANOVAS (one in each tank) revealed neither any significant difference between tanks nor between chambers.

Concentrations of organic carbon in the surface sediment (0-4 mm) samples were, given in % of dry weight, 3.9±0.3 (8 %) in tank 1 and 4.1±0.3 (7 %) in tank 2. One depth profile taken in each tank of the same parameter (data not shown), indicated a constant distribution with depth in the sediment.

Profiles of silicate concentration in the pore-water (Fig. 8 a, b) looked, in spite of some scatter especially in tank 2, similar in shape. The profiles were used to calculate outgoing fluxes by use of the methods described in Berg et al. (1998). These fluxes were 0.77 ±0.07 (9 %) mmol m^{-2} day^{-1} for tank 1 and 0.78 ±0.06 (8 %) mmol m^{-2} day^{-1} for tank 2. However, as stated in section 2.5. the overlying water in tank 1 was exchanged at an earlier stage (10 days before), relative to the time of sampling of the pore-water profiles, than in tank 2 (7 days before). Hence, the Si-concentration in the overlying water was lower in tank 2 (14.8 µM compared to 26.0 µM in tank 1). Statistical comparison (using ANOVA) of the calculated Si-fluxes indicated no significant differences between tank 1 and tank 2 and no differences between sites within the tanks. As a conclusion from the above given results the sediment mixing procedure can be considered to have been successful and the incubated sediment in each chamber at each occasion can be regarded as homogenous, within the given statistical limits.

Unless a chamber was leaking or had a malfunctioning/non-working water mixing system (insufficient to mix up the injected Br^-), the chamber volumes obtained from Br^- dilution measurements were of good quality and consistent with rough ruler controls. Following the injection, the first sample was taken after a time twice as long as the mixing time (obtained from workstation 1, Table 1). Probably because the injected Br^--solution was denser (density 1.34 kg/dm^3 in tank 1 and 1.24 kg/dm^3 in tank 2) than the chamber water (density 1.03 kg/dm^3) and sunk to the bottom, the concentration of the first sample was, in several cases, considerably lower than expected. For chambers showing this behavior the volume was calculated from the second sample, when the Br^- injection had been completely mixed with the chamber water, or from an average of the following samples (see Table 1 for chamber volumes).

Measured Si-effluxes, both from the incubations in tank 1 (incubation 1A) and the first incubations in tank 2 (incubation 2A), were initially (the four first samples) constant and then tended to level out (see Fig. 9 for typical data from the three tanks). As a consequence, for incubations 1A and 2A, the initial (first four) values were chosen for all chambers (except for three of the chambers) to calculate the Si-efflux. For the three "exception chambers" there was no clear initial slope and the correlation coefficients (r) were significantly higher if choosing all data points instead of the initial slope. For the second incubation in tank 2 (incubation 2B) the increase of Si in all chambers was constant and in every single case all data points were used to calculate the Si-effluxes (Table 1 and Fig. 9). For all three incubations, replicates (three in tank 1 and four in tank 2) of the GÖTEBORG 1 chamber were incubated in parallel. The variation in-between these chambers for incubations 1A, 2A and 2B were 12 %, 27 %, 11 %, respectively (SD/mean). The Si-effluxes for the individual chambers varied from a low 0.24 mmol m^{-2} day^{-1} for the LINKE chamber to a high 1.01 mmol m^{-2} day^{-1} for one of the GÖTEBORG 1 replicates in incubation 1A. Excluding the LINKE chamber the fluxes in incubation 1A ranged from 0.48

to 1.01 mmol m^{-2} day^{-1} with an average of 0.76 ± 0.16 mmol m^{-2} day^{-1} (21 %). For incubations in tank 2 the effluxes ranged from 0.26 to 0.71 mmol m^{-2} day^{-1} with an average of 0.43 ± 0.13 mmol m^{-2} day^{-1} (30 %, for incubation 2A) and from 0.24 to 0.40 mmol m^{-2} day^{-1} with an average of 0.32 ± 0.05 mmol m^{-2} day^{-1} (16 %, for incubation 2B, see Table 1).

Differences in silicate fluxes between the three different incubations in this study were tested for 8 different chamber designs in a two factor ANOVA and in three one factor ANOVAS within each incubation in order to test as many chambers as possible. Only the GÖTEBORG 1 chamber was replicated and the other chambers inherited their variance for each incubation. The fluxes in tank 1 were significantly higher than in tank 2 but there were no significant differences of silicate fluxes between parallel chamber incubations in each of the tanks.

Experiences from many previous oxygen uptake incubations (both *in situ* and in laboratories) have shown that uptake rates start to decrease if oxygen concentrations are allowed to drop below a certain level (e.g. Fisher et al., 1982; Hall et al., 1989). The same pattern also occurred in this study especially for some of the chambers in which the incubated water column height was low (DEVOL, DE WILDE and DUINEVELD chambers, Fig. 10). In these chambers a clear decrease in the oxygen uptake rates can be noticed. As a result, the initial slope was used to calculate the oxygen uptake. For all other chambers all data points were used (see Fig. 10 for an example). Compensations were made for the incoming water during sampling and for the BOD of the water which was on average 25 μmol l^{-1} day^{-1} in tank 1 and 21 μmol l^{-1} day^{-1} in tank 2. Due to a malfunctioning burette for Winkler titration, the quality of the data for the second incubation in tank 2 (incubation 2B) were generally too poor to be used for any evaluations of oxygen fluxes.

The replicates of the GÖTEBORG 1 chamber had oxygen fluxes within 12 % of each other for the incubations in 1A and within 14 % for the incubations 2A (SD/mean). A reverse general trend, compared to the Si-efflux, with higher oxygen uptake for all

chambers (but one) during incubation 2A compared to 1A can be distinguished (Table 1). Excluding the LINKE chamber (see above), individual fluxes ranged from 10.3 mmol m^{-2} day^{-1} for the DE WILDE chamber to 21.1 mmol m^{-2} day^{-1} for the CISE chamber with an average of 14.9 ± 3.6 mmol m^{-2} day^{-1} (25 %) in incubation 1A. In incubation 2A the fluxes were between 11.5 mmol m^{-2} day^{-1} for the DUINEVELD chamber and 22.6 mmol m^{-2} day^{-1} for one of the GÖTEBORG 1 replicates. The average for this incubation was 17.0 ± 3.2 mmol m^{-2} day^{-1} (19 %).

Statistical analyses of the oxygen flux data, in the same way as for silicate fluxes (see above), indicated that there was no significant difference between incubations (tank 1 and tank 2), but there was significant variation between chambers in each incubation. The flux of oxygen was significantly positively correlated with the height of the overlying water ($p<0.001$, $R^2=0.45$, Fig 11). None of the other of the tested factors: chamber type, chamber surface, chamber volume, chamber shape (round or squared), maximal differential pressure at the applied stirring/pumping rate, average DBL thickness, mixing time and meiofauna present in the chamber had any influence on the measured oxygen fluxes.

In spite of the fact that the initial flux rates were chosen in many of the flux calculations, a probable explanation is that chambers with a low water column height reach low oxygen concentrations more quickly, causing the fluxes to level out. This feature has been reported previously (e.g. Fisher et al., 1982; Hall et al., 1989) and shows the risk of prolonging incubations or having too low overlying water column heights in biogeochemically active sediments. If the flux rates would have been known beforehand this artifact could have been avoided by sampling chambers with low overlying water more frequently.

There have been discussions in the scientific community on appropriate chamber size. Chambers enclosing too small sediment surface areas are likely to give wall artifacts and compact the sediment when they enter. The amount of compression is dependent on

sediment penetration depth, penetration speed, sediment softness and of course, the chamber surface area. The degree of compaction was found to rapidly decrease when increasing the diameter of a cylindrical core tube (or chamber) from 34 mm to 54 mm. For a 145 mm diameter chamber, compaction effects can occur if the sediment penetration depth exceeds approximately 100 mm (Blomqvist, 1985).

The use of a large surface area chamber reduces the variability caused by small scale heterogeneity of the bottom sediment and is more likely to include a more representative number of larger animals (e.g. Glud and Blackburn, 2002). In principle the bigger surface area the better, but a bigger chamber require more space and more powerful techniques for sediment recovery. The use of multiple chambers on a lander enables controlled manipulative experiments to be carried out, replication, and/or can be an insurance if one or some of the chambers fail to work. Recommendations on which chamber size to use in sediments with various amounts of fauna can be obtained in Glud and Blackburn (2002). In addition a freely available software can be obtained for chamber users to test their particular chamber size for their particular location values of fauna and flux rates (values entered by the user). In the present study no correlation whatsoever was found between the measured fluxes and the surface area of the chambers. Hence, no wall effects were discovered even for the small (area 78 cm^2) AARHUS chamber.

4. Conclusions

- Variations in chamber design (14 designs were tested) and hydrodynamic settings did not have any statistically significant influence on the measured fluxes of oxygen and silicate in this study.

- Simple and inexpensive visualizations are a useful tool, especially for asymmetrical chambers, for initial studies of the circulation patterns in benthic chambers. Furthermore, mixing time experiments can be used to reveal at what water mixing rate there is a transition between essentially laminar and turbulent flows in a chamber.
- If using a pump for water mixing it is preferable to let the water exit through many small horizontally directed holes instead of a few big ones. When used in this way the pumps in this study gave a quick water mixing with an even distribution of bottom currents and DBL thicknesses. A disadvantage might be a higher energy demand of a pump compared to a stirrer.
- Most chambers in this study display no or low static differential pressures at the bottom when the water is mixed at rates (maximal speed$\leq$3.5 cm s^{-1}) of normal use. Consequently there is a low risk of creating stirrer induced pressure effects on the measured fluxes with the chambers presented.
- The spots where the lowest and highest absolute static pressures occurred were displaced when the stirring rates were altered in the off-center stirred chambers.
- For future chamber constructors, a design with a centrally placed stirrer is preferable since chambers with off-center placed stirrers are more difficult to map and do not seem to give any hydrodynamic advantages.
- A vertically rotating stirrer gives about 5 times lower static differential pressures at the same stirring speed as the same stirrer mounted horizontally.
- If the aim is to simulate or mimic resuspension at high flow velocities it cannot be satisfactorily done in a chamber using a horizontal (standing) rotating impeller (as is the case for most chambers in use) due to the creation of unnatural conditions, i.e. large static differential pressures and premature resuspension at certain locations in the chamber.

Acknowledgements

This intercalibration study was financed by the European Union-MAST III project "ALIPOR" under contract number CT950010. Financial support was also given by Chalmers University of Technology, Sweden and the Swedish Environmental Protection Agency. Special thanks to Berne Gustafsson for technical drawings; Magnus Malo for initial testing and development of the pressure gauges; Ingela Dahllöf and Henrik Andersson for statistical analyses and guidance; Mattias Ljungvist, Lars Bergdahl and Anders Rasmusson for scientific advice and support; Kenneth Berndtson for construction of experimental equipment; Ingrid Kubista for administrative help; and the staff at Tjärnö Marine Biological Laboratory for support and hospitality during the laboratory experiments. Constructive reviews by Will Berelson and Ken Smith improved the paper.

References

Aller, R.C., 1982. The effect of macrobenthos on chemical properties of marine sediment and overlying water. In: Animal-Sediment Relations. P.L. McCall and M.J.S. Tevesz editors, Plenum, New York, USA, 53-102.

Aller, R.C., Aller, J.Y., 1992. Meiofauna and solute transport in marine muds. Limnol. Oceanogr., 37: 1018-1033.

Aller, R.C., Hall, P.O.J., Rude, P.D., Aller J.Y., 1998. Biogeochemical heterogeneity and suboxic diagenesis in hemipelagic sediments of the Panama Basin. Deep-Sea Res., 45: 133-165.

Archer, D., Emerson, S., Smith C.R., 1989. Direct measurements of diffusive sublayer at the deep sea floor using oxygen microelectrodes. Nature, 340: 623-626.

Berelson, W.M., Hammond, D.E., 1986. The calibration of a new free-vehicle benthic flux chamber for use in the deep sea. Deep-Sea Res., 33: 1439-1454.

Berelson, W.M., Hammond, D.E., O'Neill, D., Xu, X-M., Chin, C., Zukin J., 1990. Benthic fluxes and pore water studies from sediments of the central equatorial north Pacific: Nutrient diagenesis. Geochim. Cosmochim. Acta, 54: 3001-3012.

Berelson, W.M., Hammond, D.E., Smith, K.L., JR., Jahnke, R.A., Devol, A.H., Hinga, K.R., Rowe, G.T., Sayles, F. 1987. In-situ benthic flux measurement devices: bottom lander technology. Mar. Tech. Soc., 21: 26-32.

Berg, P., Risgaard-Petersen, N., Rysgaard, S., 1998. Interpretation of measured concentration profiles in sediment pore water. Limnol. Oceanogr., 43: 1500-1510.

Blomqvist, S., 1985. Reliability of core sampling of soft bottom sediments -an in situ study. Sedimentology, 32: 605-612.

Boudreau, B.P., Guinasso, N.L., jr., 1982. The influence of a diffusive sublayer on accretion, dissolution, and diagenesis at the sea floor. In: The dynamic environment at the ocean floor, K.A. Fanning and F.T. Manheim editors, Lexinton, Massachusetts, USA, pp 115-145.

Buchhholtz-ten Brink, M.R., Gust, G., Chavis, C., 1989. Calibration and performance of a stirred benthic chamber. Deep-Sea Res., 36: 1083-1101.

Christoffersen, J., Christoffersen M.R., 1976. The kinetics of dissolution of calcium sulfate dihydrate in water. J. Crystal Growth, 35(1): 79-88.

Devol, A.H., 1987. Verification of flux measurements made with in situ benthic chambers. Deep-Sea Res., 34: 1007-1026.

Dickinson, W., Sayles, F.L., 1992. A benthic chamber with electric stirrer mixing. Tech. Report WHOI-92-09, Woods Hole Oceanogr. Inst., USA, 17 pp.

Edwards, M.F., 1985. Mixing of low viscosity liquids in stirred tanks. In: Mixing in the process industries. N. Harnby, M.F. Edwards and A.W. Nienow, editors, Butterworths, Kent, England, 131-144.

Fisher, T.R., Carlson, P.R., Barber, R.T., 1982. Sediment nutrient regeneration in three North Carolina estuaries. Estuar. Coast. Shelf Sci., 14: 101-116.

Glud, R. N., Blackburn, N., 2002. The effects of chamber size on benthic oxygen uptake measurements: a simulation study. Ophelia, 56: 23-31.

Glud, R.N., Forster, S., Huettel, M., 1996. Influence of radial pressure gradients on solute exchange in stirred benthic chambers. Mar. Ecol. Prog. Ser., 141: 303-311.

Glud, R.N., Gundersen, J.K., Revsbech, N.P., Jørgensen, B.B., Huettel, M., 1995. Calibration and performance of the stirred flux chamber from the benthic lander ELINOR. Deep-Sea Res., 42: 1021-1092.

Glud, R.N., Gundersen, J.K., Jørgensen, B.B, Revsbech, N.P., Schulz, H.D., 1994. Diffusive and total oxygen uptake of deep-sea sediments in the eastern South Atlantic Ocean: in situ and laboratory measurements. Deep-Sea Res., 41: 1767-1788.

Gundersen, J.K., Jørgensen, B.B., 1990. Microstructure of diffusive boundary layers and the oxygen uptake of the sea floor. Nature, 345: 604-607.

Gust, G., 1988. Skin friction probes for field applications. J. Geophys. Res., 93: 121-132.

Gust, G., 1990. Method of generating precisely-defined wall shearing stresses. U.S. Patent No. 4,973,165,1990.

Gust, G., Müeller, V., 1997. Interfacial hydrodynamics and entrainment functions of currently used erosion devices. Cohesive Sediments. Edited by N. Burt, R. Parke and J. Watts. John Wiley, Chichester, U.K.

Gust, G., Weatherly, G.L., 1985. Velocities, turbulence, and skin friction in a deep-sea logarithmic layer. J. Geophys. Res., 90: 4779-4792.

Hall, P.O.J., Anderson, L.G., Rutgers van der Loeff, M.M., Sundby, B., Westerlund, S.F.G., 1989. Oxygen uptake kinetics in the benthic boundary layer. Limnol. Oceanogr., 34: 734-746.

Hinze, J.O., 1975. Turbulence, 2 edition, B.J. Clark editor, McGraw-Hill, New York, NY, USA, pp. 767.

Huettel, M., Gust, G., 1992a. Solute release mechanisms from confined sediment cores in stirred benthic chambers and flume flows. Mar. Ecol. Prog. Ser., 82: 187-197.

Huettel, M., Gust, G., 1992b. Impact of bioroughness on interfacial solute exchange in permeable sediments. Mar. Ecol. Prog. Ser., 89: 253-267.

Jahnke, R.A., Christiansen, M.B., 1989. A free-vehicle benthic chamber instrument for sea floor studies. Deep-Sea Res., 36: 625-637.

Jørgensen, B.B., 1983a. Processes at the sediment-water interface. In: B. Bolin and R.B. Cook editors, The Major Biogeochemical Cycles and Their Interactions. Scope, Stockholm, Sweden, pp. 477-509.

Jørgensen, B.B., Des Marais, D.J., 1990. The diffusive boundary layer of sediments: Oxygen microgradients over a microbial mat. Limnol. Oceanogr., 35: 1343-1355.

Jørgensen, B.B., Revsbech, N.P., 1985. Diffusive boundary layers and the oxygen uptake of sediments and detritus. Limnol. Oceanogr., 30: 111-122.

Jørgensen, C.B., 1983b. Fluid mechanical aspects of suspension feeding. Mar. Ecol. Prog. Ser., 11: 89-103.

Koop, K., Boynton, W.R., Wullf, F., Carman, R., 1990. Sediment - water oxygen and nutrient exchanges along a depth gradient in the Baltic Sea. Mar. Ecol. Prog. Ser., 63: 65-77.

Lenihan, H.S., Peterson, C.H., Allen, J.M., 1996. Does flow speed also have a direct effect on growth of active suspension-feeders: An experimental test on oysters. Limnol. Oceanogr., 41: 1359-1366.

Lund-Hansen, L.C., Jensen, O., Christiansen, C., Laima, M., 1999. The LABEREX chamber for studying the critical shear stress for fine-grained sediment. Danish J. Geogr., 99: 1-7.

Lund-Hansen, L.C., Laima, M., Mouritsen, K.N., Lam, Y., Hai, A., 2002. Effects of benthic diatoms, fluff layer, and sediment conditions on critical shear stress in a non-tidal coastal environment. J. Mar. Biol. Assoc., U.K., 82: 1-8.

Martin, W.R., Banta, G.T., 1992. The measurements of sediment irrigation rates: a comparison of the Br^- tracer and $^{222}Rn/^{226}Rn$ disequilibrium techniques. J. Mar. Res., 50: 125-154.

McIntyre, A.D., Warwick, K.M., 1984. Meiofauna techniques. In: Methods for the study of marine benthos, N.A. Holme and A.D. McIntyre, editors, Blackwell Scientific Publications, Oxford: 217-244.

Murray, J.W., Emerson, S., Jahnke, R., 1980. Carbonate saturation and the effect of pressure on the alkalinity of interstitial waters from the Guatemala Basin. Geochim. Cosmochim. Acta, 44: 963-972.
Opdyke, B.N., Gust, G., Ledwell, J.R., 1987. Mass transfer from smooth alabaster surfaces in turbulent flows. Geophys. Res. Let., 14: 1131-1134.
Poisson, A., Papaud, A., 1983. Diffusion coefficients of major ions in seawater. Mar. Chem., 13: 265-280.
Rutgers van der Loeff, M.M., Anderson, L.G., Hall, P.O.J., Iverfeldt, Å., Josefson, A.B., Sundby, B., Westerlund, S.F.G., 1984. The asphyxiation technique: An approach to distinguishing between molecular diffusion and biologically mediated transport at the sediment-water interface. Limnol. Oceanogr., 29: 675-686.
Santschi, P.H., Andersson, R.F., Fleisher, M.Q., Bowles, W., 1991. Measurements of diffusive sublayer thickness in the ocean by alabaster dissolution, and their implications for the measurements of benthic fluxes. J. Geophys. Res., 96: 10641-10657.
Santschi, P.H., Bower, P., Nyffeler, U.P., Azevedo, A., Broecker, W.S., 1983. Estimates of the resistance to chemical transport posed by the deep-sea boundary layer. Limnol. Oceanogr., 28: 899-912.
Santschi, P.H., Nyffeler, U.P., O´Hara, P., Buchholtz-ten-Brink, M., Broecker, W.S., 1984. Radiotracer uptake on the sea floor: results from the MANOP chamber deployments in the eastern Pacific. Deep-Sea Res., 31: 451-468.
Sayles, F.L., Dickinson, W.H., 1991. The ROLAI^{2}D lander: a benthic lander for the study of exchange across the sediment-water interface. Deep-Sea Res., 38: 505-529.
Sayles, F.L., Martin, R., 1995. In situ tracer studies of solute transport across the sediment-water interface at the Bermuda Time Series site. Deep-Sea Res., 42: 31-52.
Shaw, J.A., 1994. Understand the effects of impeller type, diameter, and power on mixing time. Chem. Engineer. Prog., 90(2): 45-48.
Snedecor, G.W., Cochran, W.G., 1967. Statistical methods. University of Iowa Press, Ames IA, 6th edition, USA, pp 593.
Strickland, J.D.N., Parson, T.R., 1968. A practical hand-book of seawater analysis. Bull. Fish Res. Border Canada, 167: 311 pp
Tengberg, A., de Bovée, F., Hall, P., Berelson, W., Chadwick, D., Ciceri, G., Crassous, P., Devol, A., Emerson, S., Gage, J., Glud, R., Graziottin, F., Gundersen, J., Hammond, D., Helder, W., Hinga, K., Holby, O., Jahnke, R., Khripounoff, A., Lieberman, S., Nuppenau, V., Pfannkuche, O., Reimers, C., Rowe, G., Sahami, A., Sayles, F., Schurter, M., Smallman, D., Wehrli, B., de Wilde, P., 1995. Benthic chamber and profiling landers in oceanography - A review of design, technical solutions and functioning. Prog. Oceanogr., 35: 253-292.
Tengberg, A., Stahl, H., Gust, G., Muller, V., Arning, U., Andersson, H., Hall, POJ., 2004. Intercalibration of benthic flux chambers I. Accuracy of flux measurements and influence of chamber hydrodynamics. Prog. Oceanogr., in press.
Underwood, A. J., 1997. Experiments in Ecology, Their logical design and interpretation using analysis of variance. Cambridge University Press, Cambridge.
Vershinin, A.V., Gornizkij, A.B., Egorov, A.V., Rozanov, A.G., 1994. The method of investigation of chemical exchange across the water-sediment interface in open sea-bottom systems. Okeanologia, 34: 139-145.
Vogel, S., 1981. Life in moving fluids: the physical biology of flow. Willard Grant, Boston, USA.

FIGURE CAPTIONS

Fig.1. Scaled (approximate scale 1:5 except for chamber number 14 (LINKE) for which the approximate scale is 1:10) drawings of the fourteen participating chambers showing the size and shape of the chambers as well as of the water mixing mechanisms (stirrers/pumps) and the main hydrodynamic obstacles (e.g. electrodes and water-sampling systems). The small circular spots indicate locations where static pressure was measured and the filled squares the size and position (and number) of alabaster plates in each chamber. The emplacement and size of LDA measurement grids have also been included but no data from these measurements are treated in this paper.

Fig.2. Emplacement of the chambers and the location of different samples taken to test the homogeneity of sediment (particulate C and N, dissolved Si-profiles and meiofauna) for the parallel flux incubations in tank 1.

Fig.3. Emplacement of the chambers and the location of different samples taken to test the homogeneity of sediment (particulate C and N, dissolved Si-profiles and meiofauna) for the parallel flux incubations in tank 2.

Fig.4A. The water movement in a symmetrically stirred chamber can be divided into three main characteristic features: rotation around the main vortex axis, separation below and above the stirrer and suction into the impeller through the main vortex.

Fig.4B. In an asymmetrically stirred chamber the vortex rises diagonally (example from the GÖTEBORG 1 chamber).

Fig.4C. If using a pump with few outlet holes instead of many small ones (diffuser) there is a risk of creating an uneven distribution of current speeds in the chamber (example from the DE WILDE chamber).

Fig.5. Mixing time as a function of stirring rate for the GÖTEBORG 1 chamber.

Fig.6. Static pressures in the CISE chamber measured at eight locations with a stirring speed of 10 RPM and with four stirring bars mounted. Pressure gauge number 1 was

measuring a negative pressure and was placed in the center where the vortex was rising. Gauge number 8 was located in the periphery close to the chamber wall and was measuring a slight positive pressure. The maximal differential pressure at this occasion was 3.4 Pa. Note that pressure gauge number 6 is malfunctioning.

Fig.7. Calcium concentration increase with time in the overlying water during alabaster plate experiments in seven different chambers. Please note that the ratio exposed alabaster surface/chamber volume is different for the different chambers giving rise to different concentration increases. The experiments were done at 19.0 ± 1° C.

Fig.8A. Silicate porewater concentration against sediment depth. Seven profiles were collected at different locations in tank 1.

Fig.8B. Silicate porewater concentration against sediment depth. Six profiles were collected at different locations in tank 2.

Fig.9. Typical silicate concentration with time given for three different chambers at three different tank experiments.

Fig.10. Oxygen concentration with time in the DEVOL and WITTE chambers during incubation 2A. Observe that for the DEVOL chamber the initial (the first four data points) uptake is higher than later during the incubation.

Fig.11. Oxygen uptake for individual chambers plotted against overlying water column height for all the incubations. Oxygen flux is correlated to the chamber water height, the solid line is the least squares regression with 95% confidence intervals indicated by the dotted lines.

Table 1

CHAMBER #	STATION 1 Stirring speed/ pump flow	STATION 1 Mixing time [s]	STATION 2 Max diff. pressure [Pa]	STATION 3 Stirring rate and average DBL [µm]	STATION 3 Average DBL above individual plates (calculated from weight loss) [µm]	[µm]	[µm]	[µm]	[µm]	[µm]	STATION 4 Incubation # and (stirring) (rate)	Volume [ml] and overlying water height [cm] (from Br)	Sediment oxygen uptake [mmol/m2*day]	Sediment silica efflux [mmol/m2*day]
1 GÖTE1	8 RPM 10 RPM 21 RPM 40 RPM 87 RPM	120 60 35	0.5 2.5 9.6	10 RPM **486±84**	483 (A7)	587 (A14)	494 (A9)	381 (A8)			1A (10 RPM) 2A (10 RPM) 2B (10 RPM)	various various various	17,2±2,1* 19,3±2,7**	0,893±0,11* 0,309±0,08** 0,317±0,04**
2 GÖTE2	9 RPM 20 RPM 40 RPM 86 RPM	150 30	0.7 2.0 7.6	No alabaster							No incubations			
3 BANYULS	30 RPM	about 3600	<0,3	No alabaster							No incubations			
4 IFREMER	3 RPM 7 RPM	1200 240	<0,3	7 RPM **711±169**	595 (A22)	703 (A20)	963 (A2)	767 (A25)	526 (A15)		1A (7 RPM) 2A (7 RPM) 2B (7 RPM)	12 530; 17,9 11 976; 17,1 11 976; 17,1	12,3 15,9	0.704 0.521 0.322
5 ROWE	110 RPM 50 ml/s 110 RPM+50 ml/s	85 42 38	0.6 1.5 2.2	110 RPM & 50 ml/s **362±84**	481 (B4)	306 (B5)	387 (B6)	377 (B7)	261 (B8)		No incubations			
6 AARHUS	8 RPM 20 RPM 34 RPM 68 RPM	46 29	0.7 7.5 27.0	No alabaster							1A (12 RPM) 2A (9 RPM) 2B (10 RPM)	1004; 12,8 873; 11,1 873; 11,1	11,8 14,9	0.765 0.431 0.283
7 BMIC	288 RPM	87	<0,3	288 RPM **332±67**	358 (B2)	382 (A18)	255 (A19)				No incubations			
8 DUINEV	13 ml/s 15 ml/s 17 ml/s	600 355 132	<0,4	15 ml/s **710±253**	484 (C1)	796 (C2)	530 (C3)	1029 (C4)			2A (17 ml/s) 2B (17 ml/s)	1228; 8,5 1228; 8,5	11.5	0.358 0.242
9 WITTE	60 RPM 120 RPM	120 50	0.4 0.8	60 RPM **474±56**	391 (A6)	495 (A3)	513 (A4)	497 (A5)			1A (50 RPM) 2A (50 RPM) 2B (50 RPM)	5262; 13,2 4596; 11,5 4596; 11,5	10.6 15.2	0.669 0.535 0.341
10 DEVOL	60 RPM	240	<0,3	No alabaster							1A (60 RPM) 2A (60 RPM) 2B (60 RPM)	4116; 10,3 2956; 7,4 2956; 7,4	15.7 17.3	0.568 0.468 0.358
11 DE WILDE	37 ml/s 60 ml/s	120 60	<0,4	60 ml/s **426±112** **413±112**	429 (D1) 426 (D11)	445 (D2) 433 (D12)	436 (D3) 440 (D13)	568 (D4) 538 (D14)	253 (D5) 230 (D15)		1A (60 ml/s) 2A (60 ml/s) 2B (60 ml/s)	5939; 7,3 5085; 6,2 5085; 6,2	10.3 12.6	0.484 0.425 0.397
12 NAVAL COMMAND	5 ml/s 10 ml/s 15 ml/s	480 270 120	<0,3	15 ml/s **401±72**	360 (A24)	474 (A21)	456 (A23)	299 (A1)	415 (A26)		1A (15 ml/s) 2A (15 ml/s) 2B (15 ml/s)	39 744; 24,8 42 128; 26,3 42 128; 26,3	15.2 19.5	0.895 0.714 0.368
13 CISE	10RPM; 1 bar 10RPM; 2 bars 10RPM; 4 bars	135 135 135	1.3 2.1 3.4	10 (1 bar) **294±26**	322 (A13)	294 (A27)	301 (A8)	318 (A3)	277 (A2)	254 (A10)	1A (10RPM, 2 bars) 2A (10RPM,2 bars) 2B (10RPM, 2 bars)	112 728; 29,3 126 588; 32,9 126 588; 32,9	21.1 19.6	0.883 0.436 0.242
14 LINKE	60 RPM 70 RPM 86 RPM	480 180 120	No pressure	No alabaster							1A (81 RPM)	164 802; 13,6	9.3	0.241

Table 1: Individual results for each of the chamber designs including: stirring rate and/or pump flow, mixing time, maximal differential pressure, average Diffusive Boundary Layer Thickness (DBL, from alabaster plates), DBL for each of the individual alabaster plates and flux incubation results (oxygen and silicate) from three incubations (1A, 2A and 2B)

* Results from three parallel incubations
** Results from four parallel incubations

Fig 1

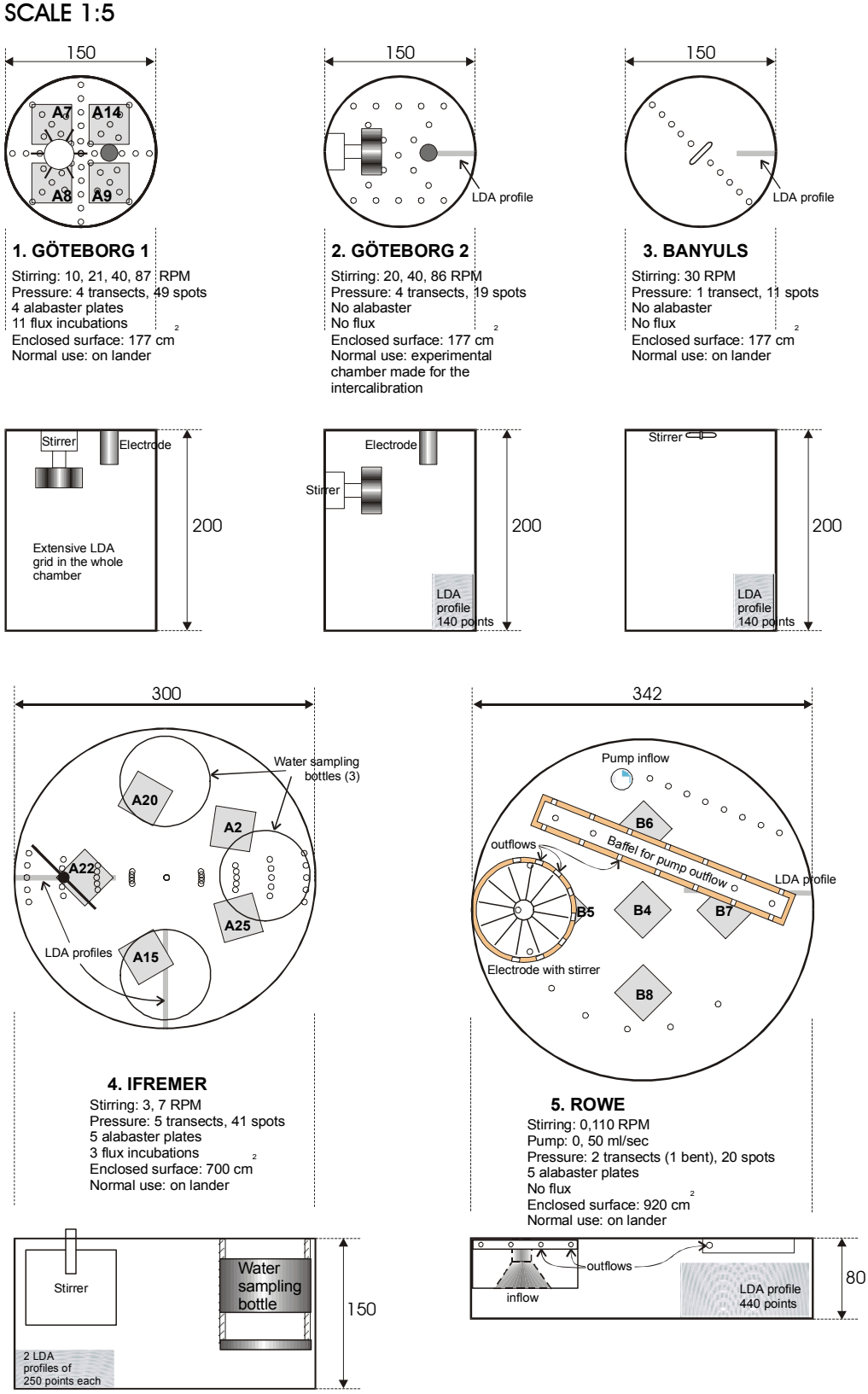
SCALE 1:5
150
A7
A14
A8
A9
1. GÖTEBORG 1
Stirring: 10, 21, 40, 87 RPM
Pressure: 4 transects, 49 spots
4 alabaster plates
11 flux incubations
Enclosed surface: 177 cm2
Normal use: on lander
150
LDA profile
2. GÖTEBORG 2
Stirring: 20, 40, 86 RPM
Pressure: 4 transects, 19 spots
No alabaster
No flux
Enclosed surface: 177 cm2
Normal use: experimental chamber made for the intercalibration
150
LDA profile
3. BANYULS
Stirring: 30 RPM
Pressure: 1 transect, 11 spots
No alabaster
No flux
Enclosed surface: 177 cm2
Normal use: on lander
Stirrer
Electrode
200
Extensive LDA grid in the whole chamber
Electrode
Stirrer
200
LDA profile 140 points
Stirrer
200
LDA profile 140 points
300
Water sampling bottles (3)
A20
A2
A22
A25
LDA profiles
A15
4. IFREMER
Stirring: 3, 7 RPM
Pressure: 5 transects, 41 spots
5 alabaster plates
3 flux incubations
Enclosed surface: 700 cm2
Normal use: on lander
Stirrer
Water sampling bottle
150
2 LDA profiles of 250 points each
342
Pump inflow
B6
outflows
Baffel for pump outflow
LDA profile
B5
B4
B7
Electrode with stirrer
B8
5. ROWE
Stirring: 0,110 RPM
Pump: 0, 50 ml/sec
Pressure: 2 transects (1 bent), 20 spots
5 alabaster plates
No flux
Enclosed surface: 920 cm2
Normal use: on lander
outflows
inflow
LDA profile 440 points
80

Fig 1

SCALE 1:5

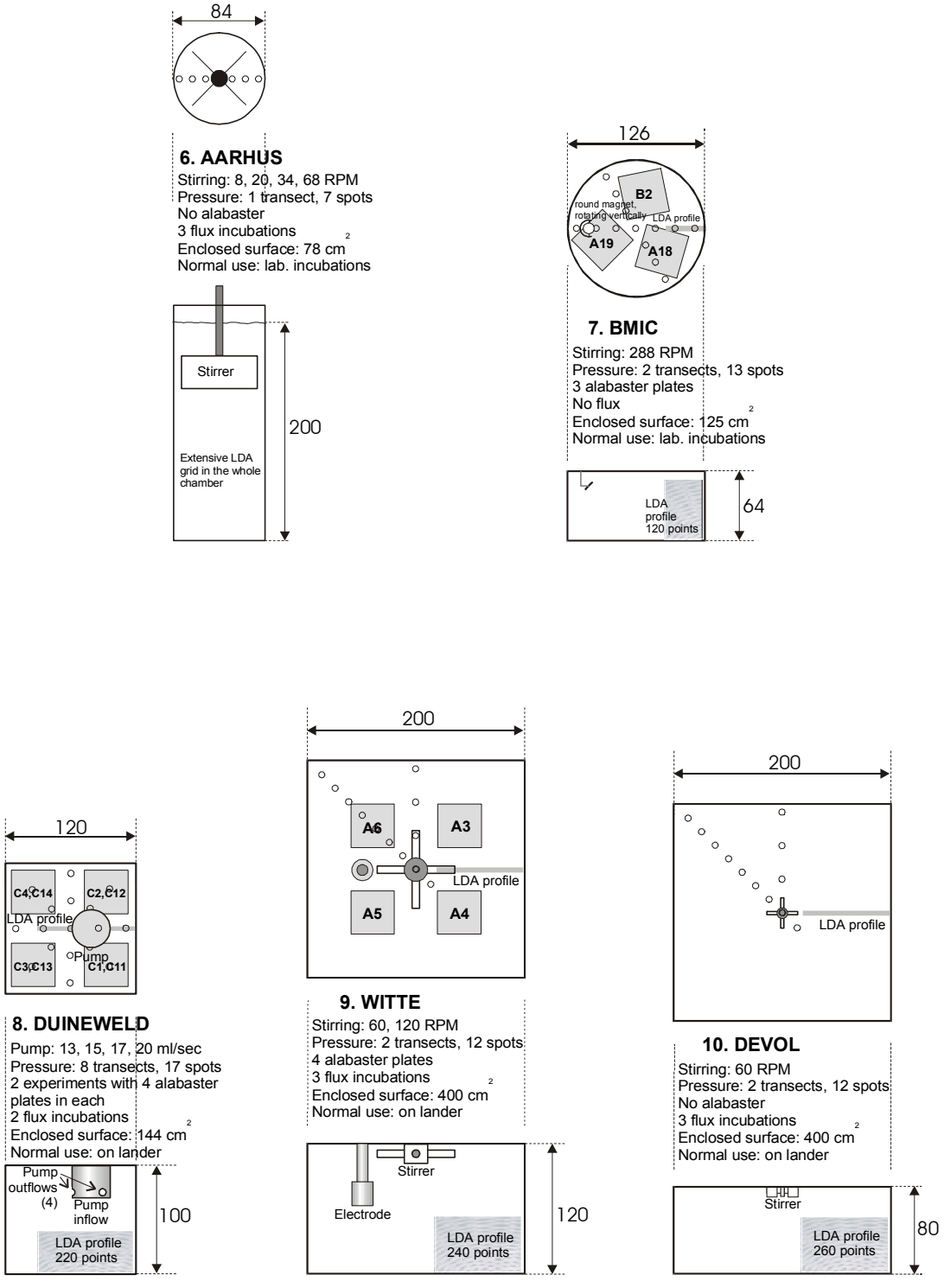

Fig 1

SCALE 1:5

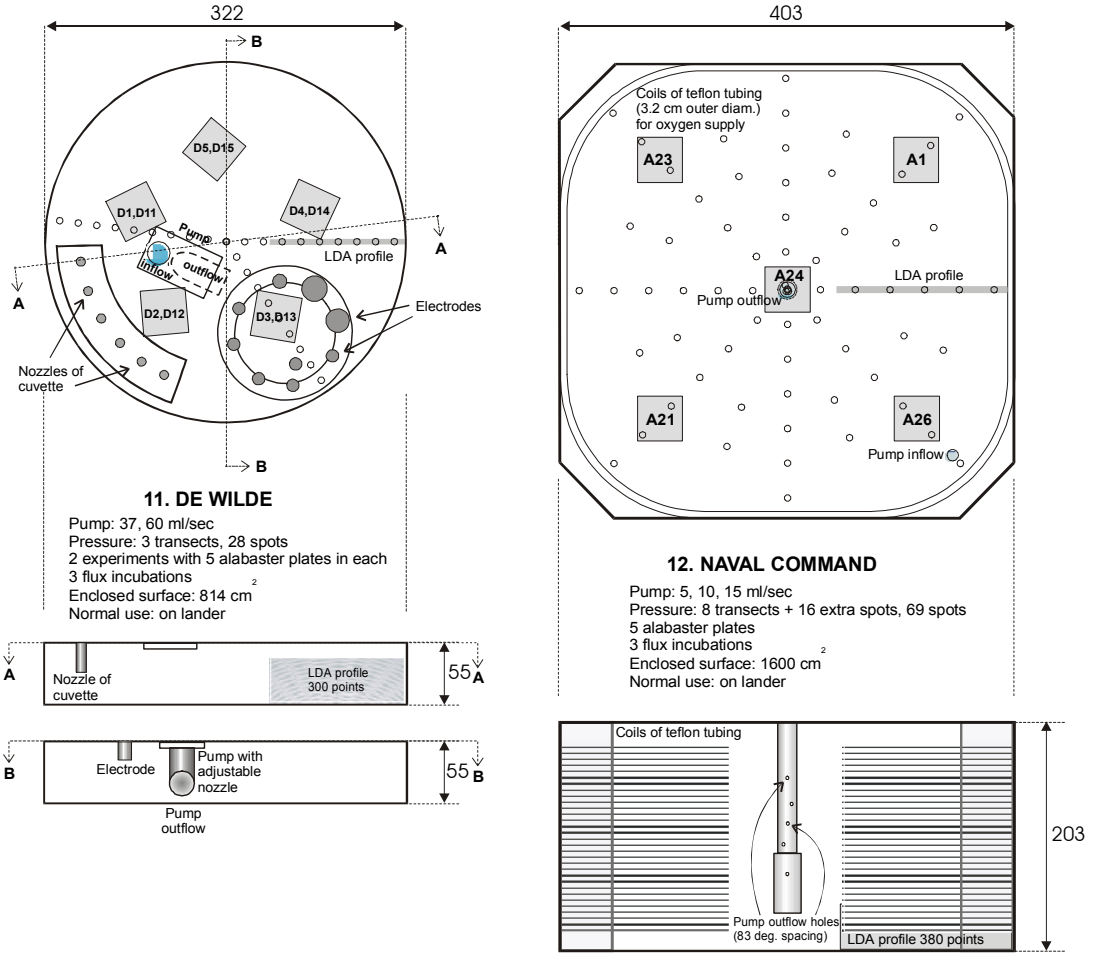

Fig 1

SCALE 1:5

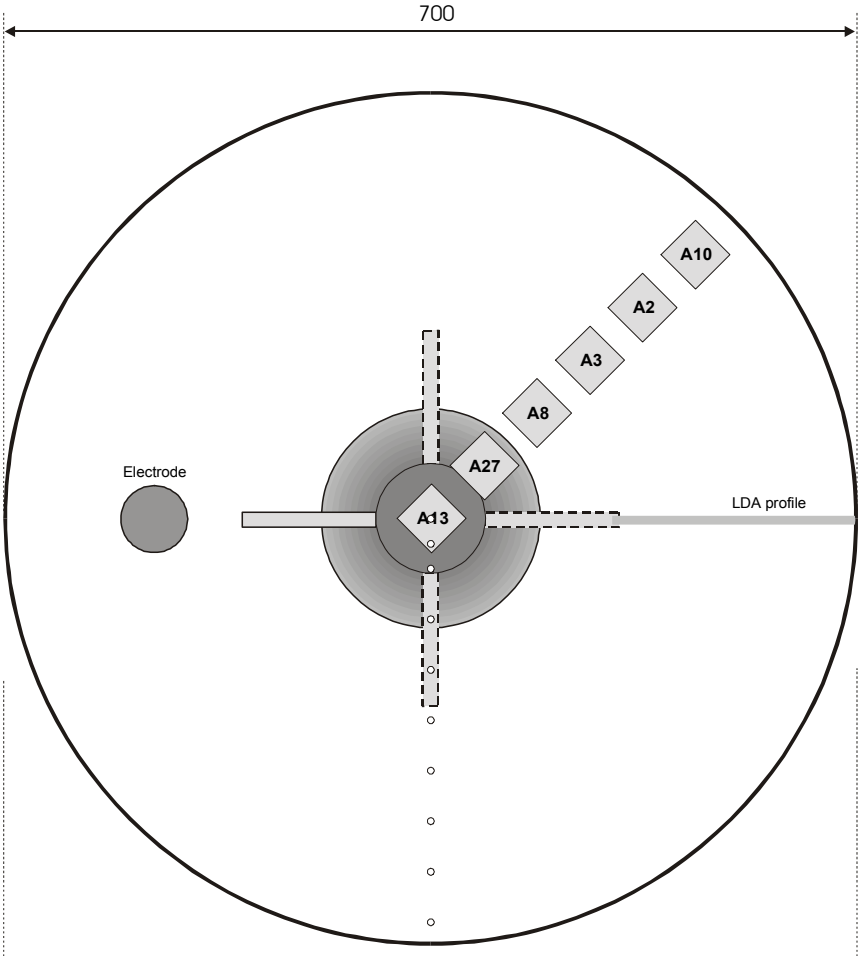

13. CISE

Stirring: 10 RPM with 1 to 4 bars
Pressure: 1 transect, 10 spots
6 alabaster plates
3 flux incubations
Enclosed surface: 3850 cm^2
Normal use: on lander

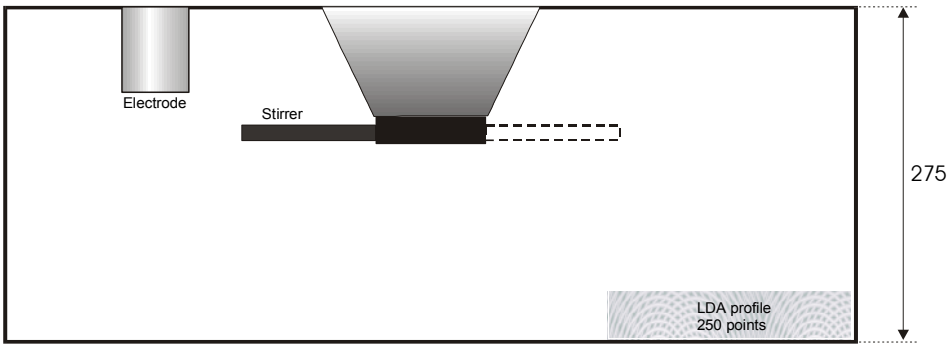

Fig 1

SCALE 1:10

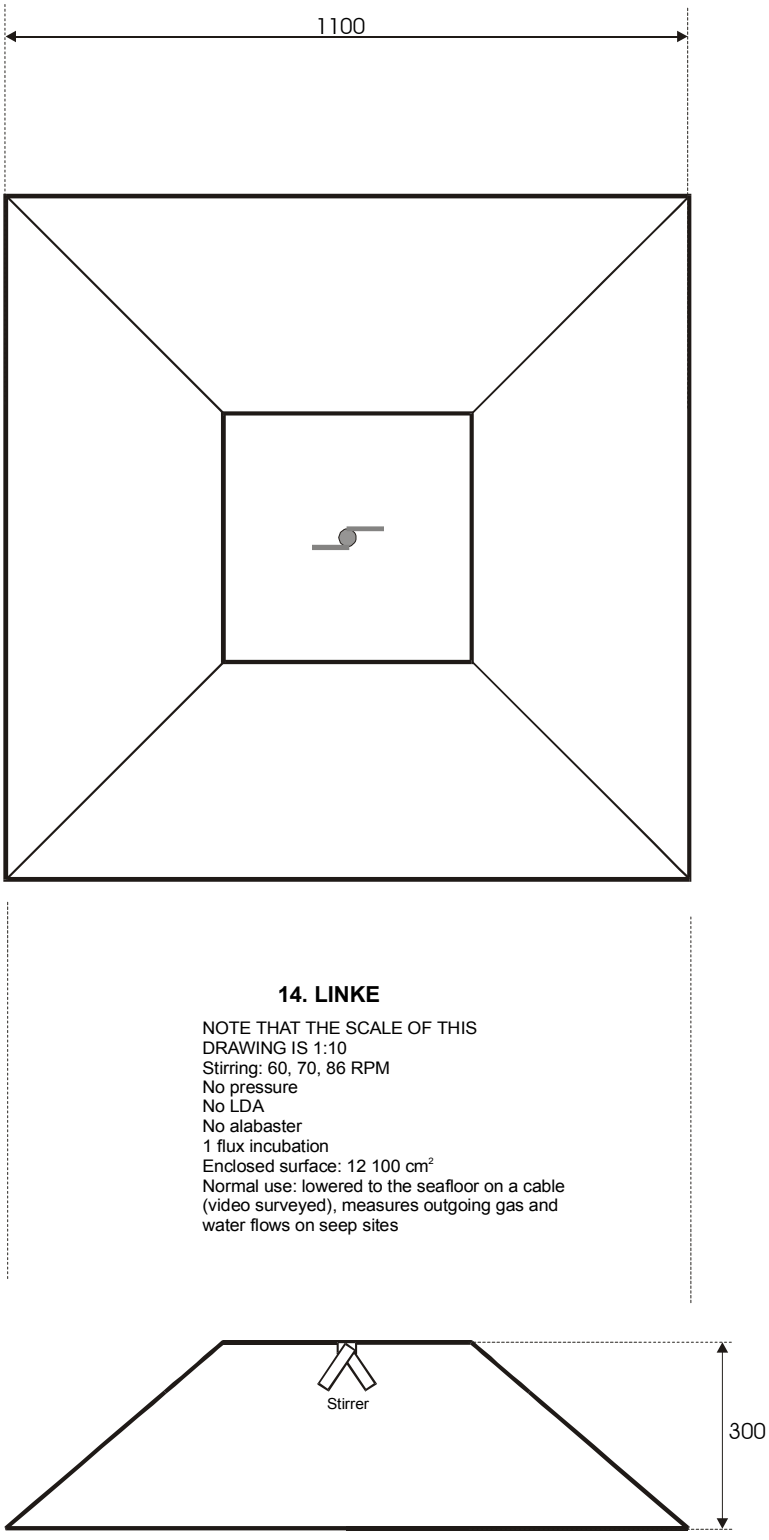

Fig 2

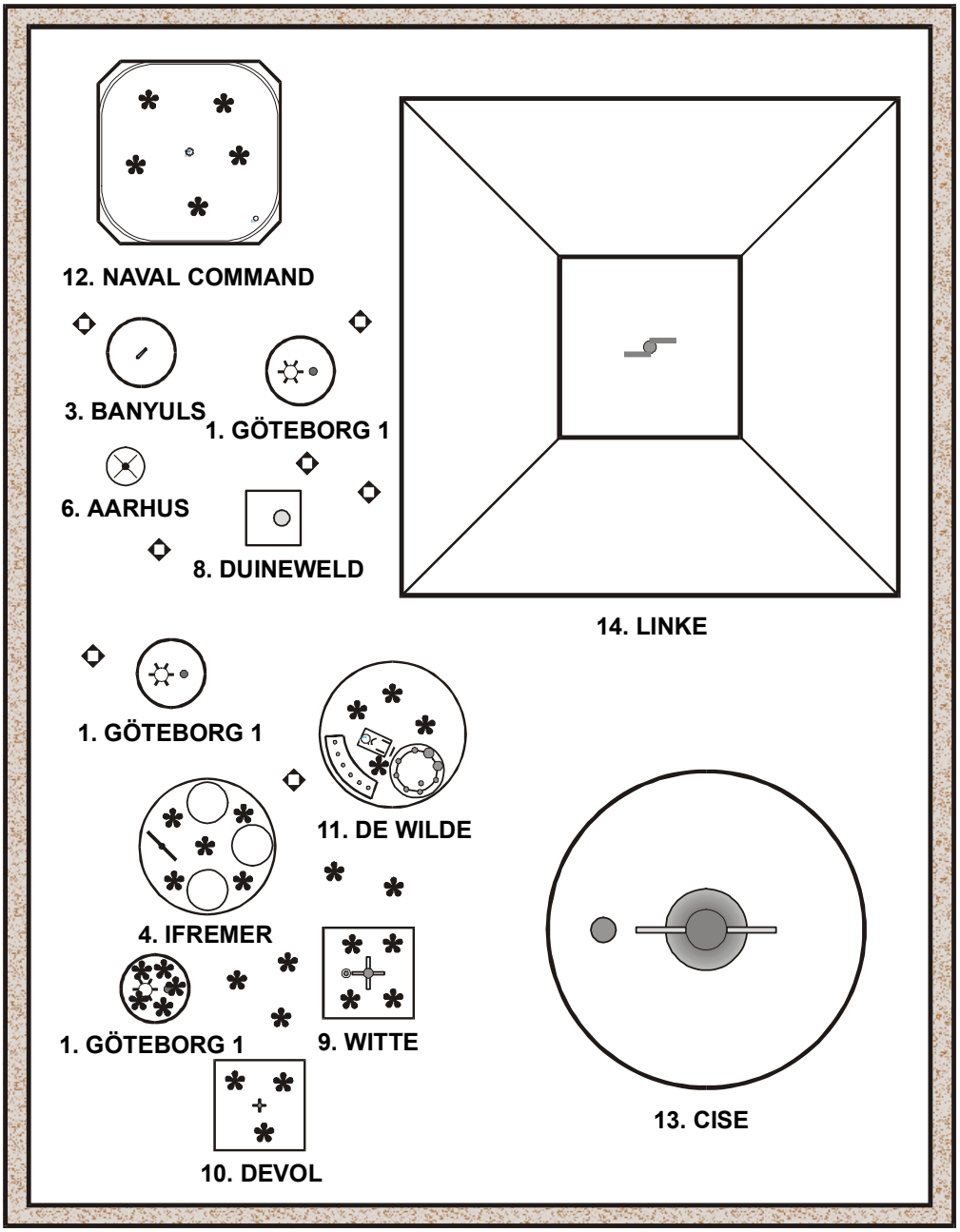

* Meiofauna sample
◇ Si-profile, C and N sample

Fig 3

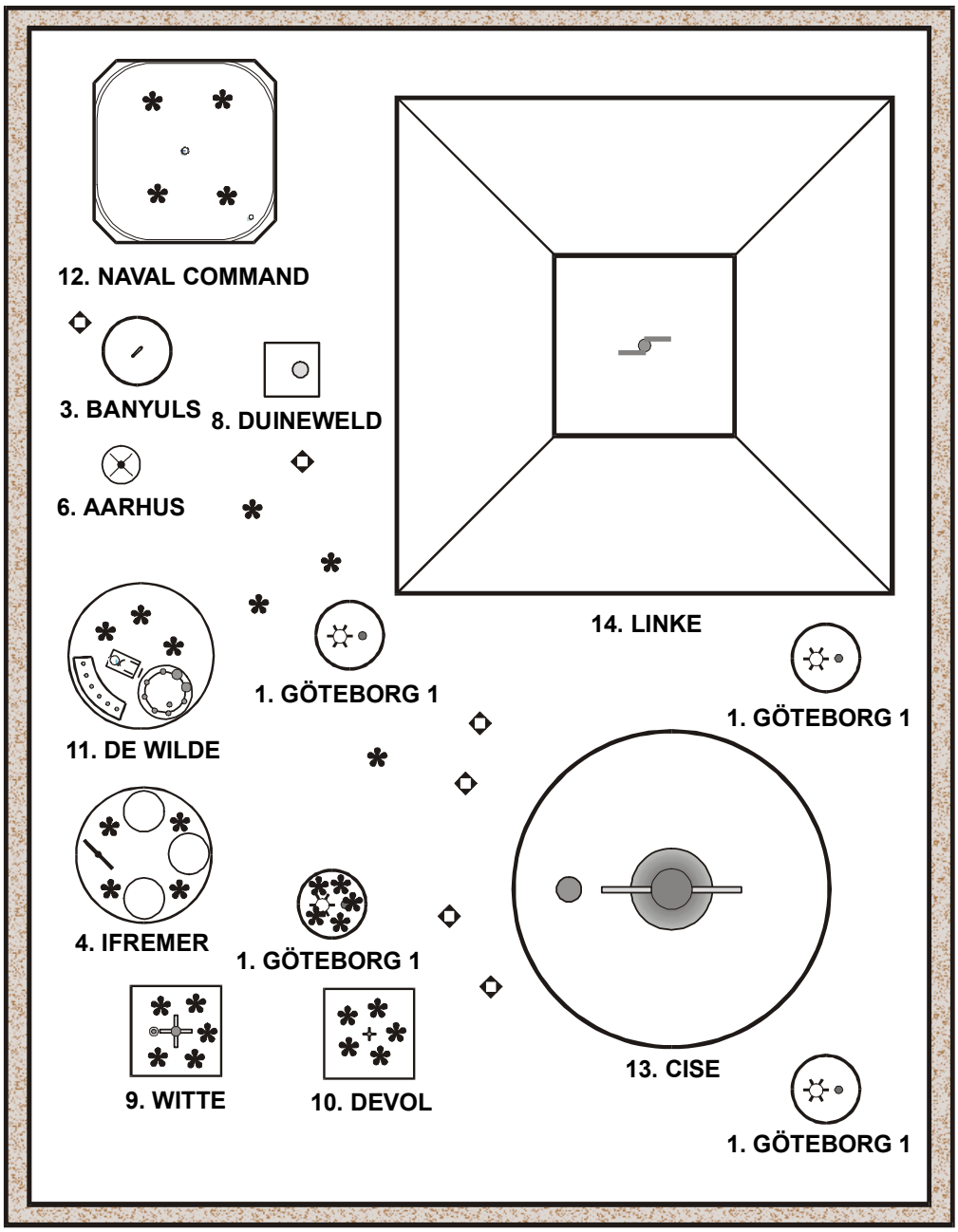
12. NAVAL COMMAND
3. BANYULS
8. DUINEWELD
6. AARHUS
14. LINKE
1. GÖTEBORG 1
1. GÖTEBORG 1
11. DE WILDE
4. IFREMER
1. GÖTEBORG 1
13. CISE
9. WITTE
10. DEVOL
1. GÖTEBORG 1
Meiofauna sample
Si-profile, C and N sample

Fig 4

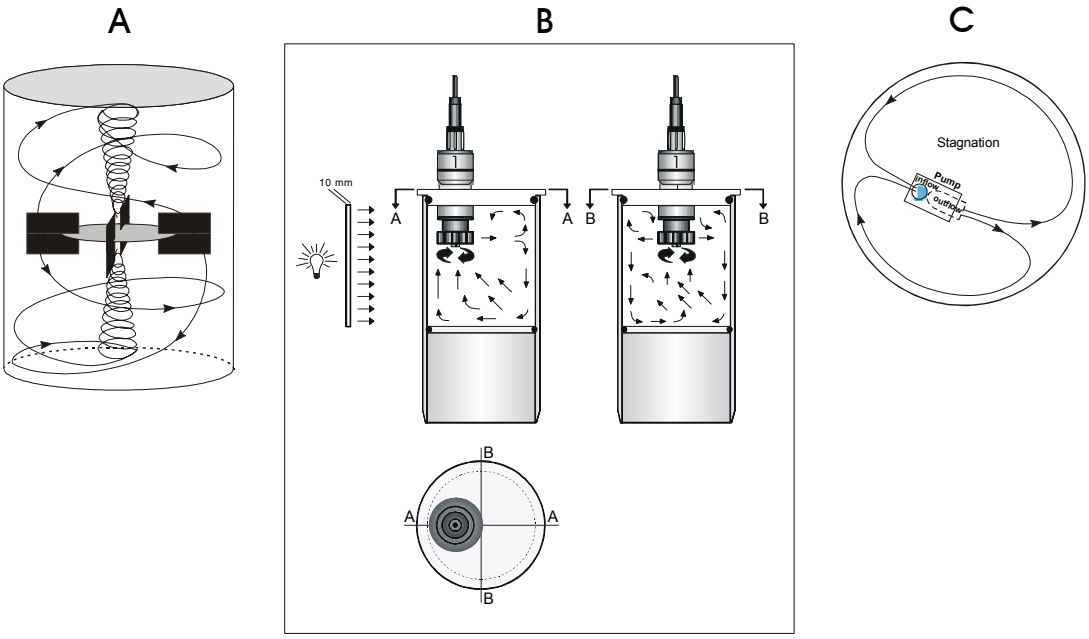

Fig 5

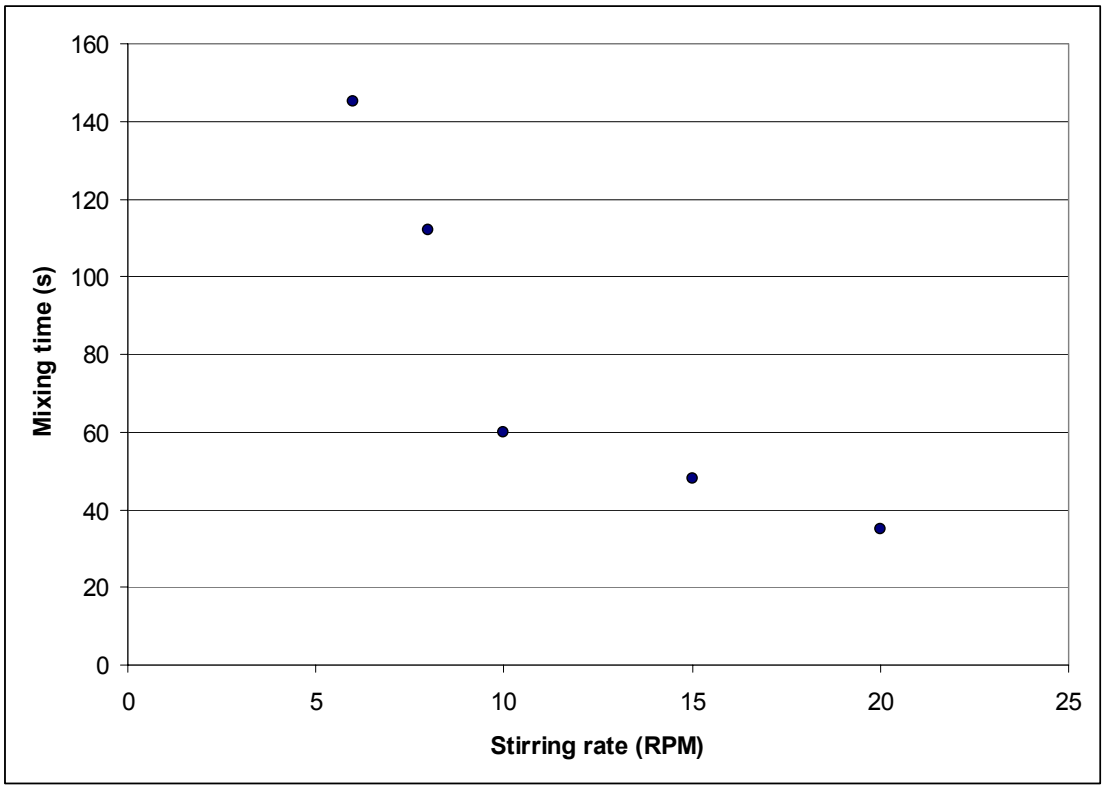
160
140
120
100
80
60
40
20
0
Mixing time (s)
0
5
10
15
20
25
Stirring rate (RPM)

Fig 6

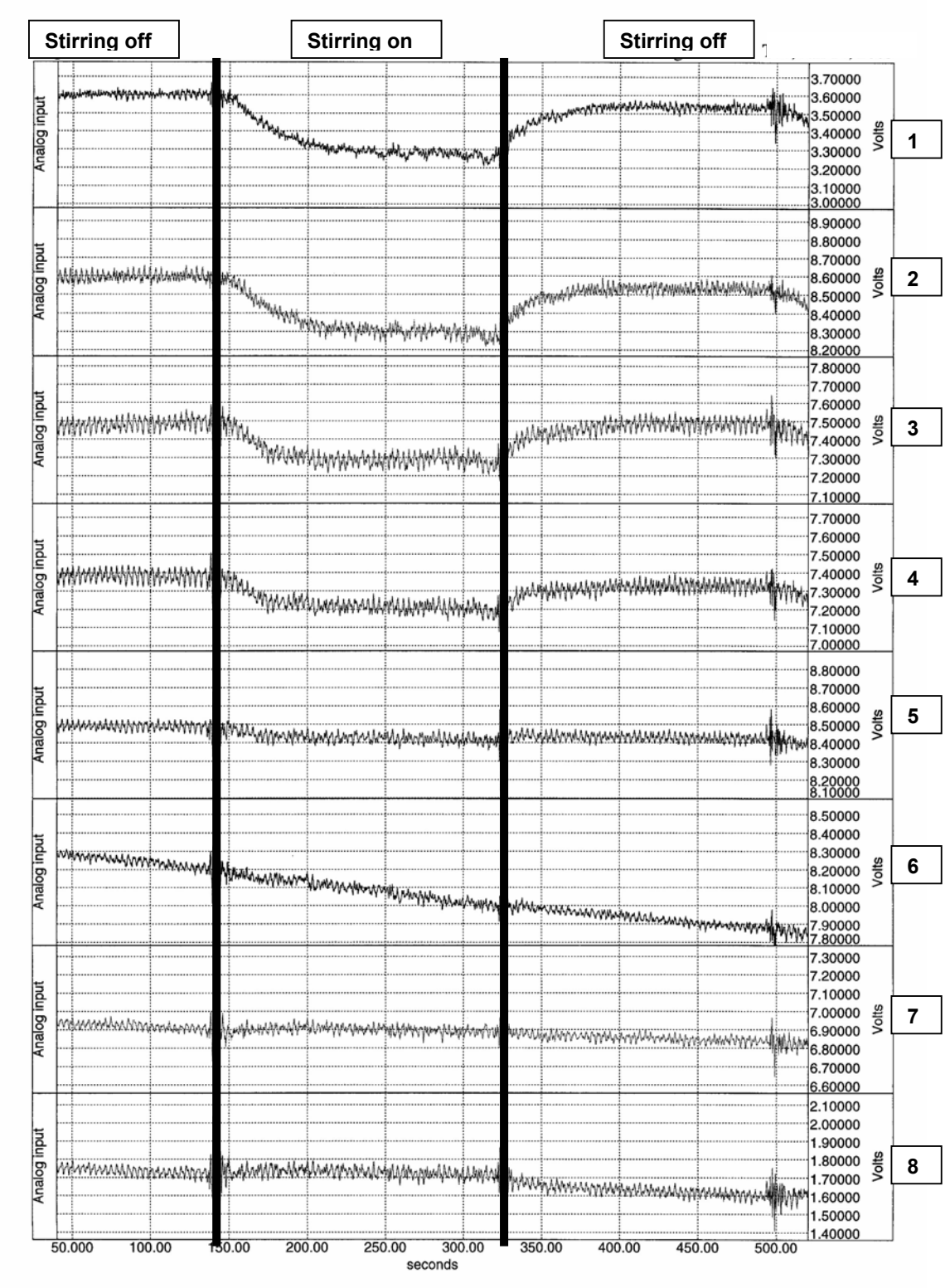
Stirring off
Stirring on
Stirring off
Analog input
Volts
1
2
3
4
5
6
7
8
50.000
100.00
150.00
200.00
250.00
300.00
350.00
400.00
450.00
500.00
seconds

Fig 7

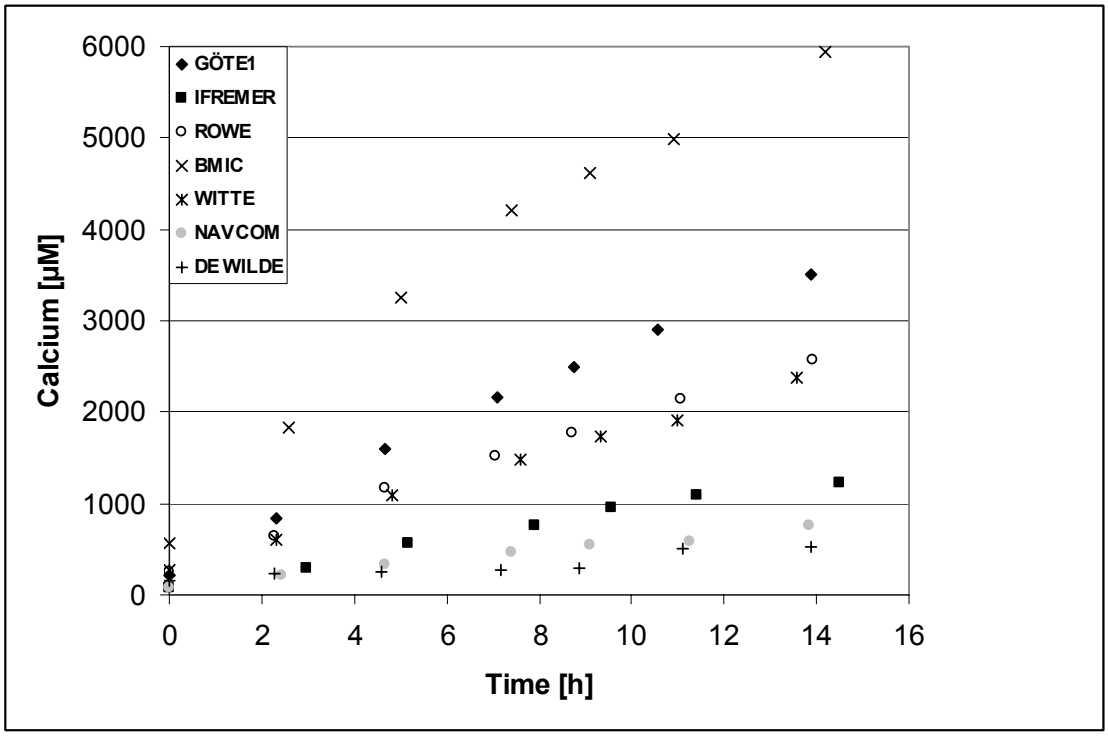
GÖTE1
IFREMER
ROWE
BMIC
WITTE
NAVCOM
DE WILDE
Calcium [µM]
Time [h]
0
1000
2000
3000
4000
5000
6000
0
2
4
6
8
10
12
14
16

Fig 8

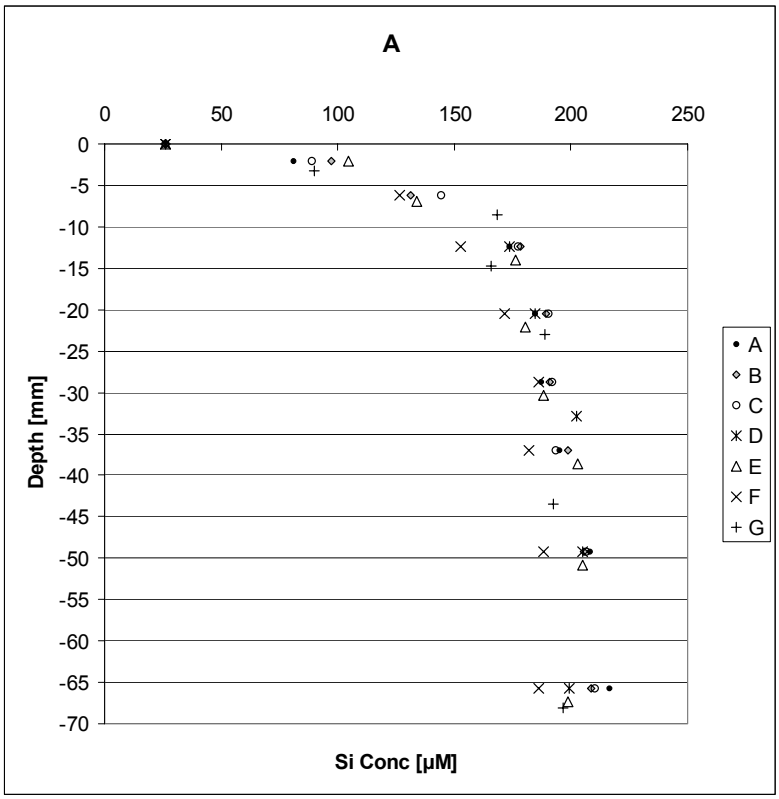
A
0
50
100
150
200
250
0
-5
-10
-15
-20
-25
-30
-35
-40
-45
-50
-55
-60
-65
-70
Depth [mm]
Si Conc [µM]
A
B
C
D
E
F
G

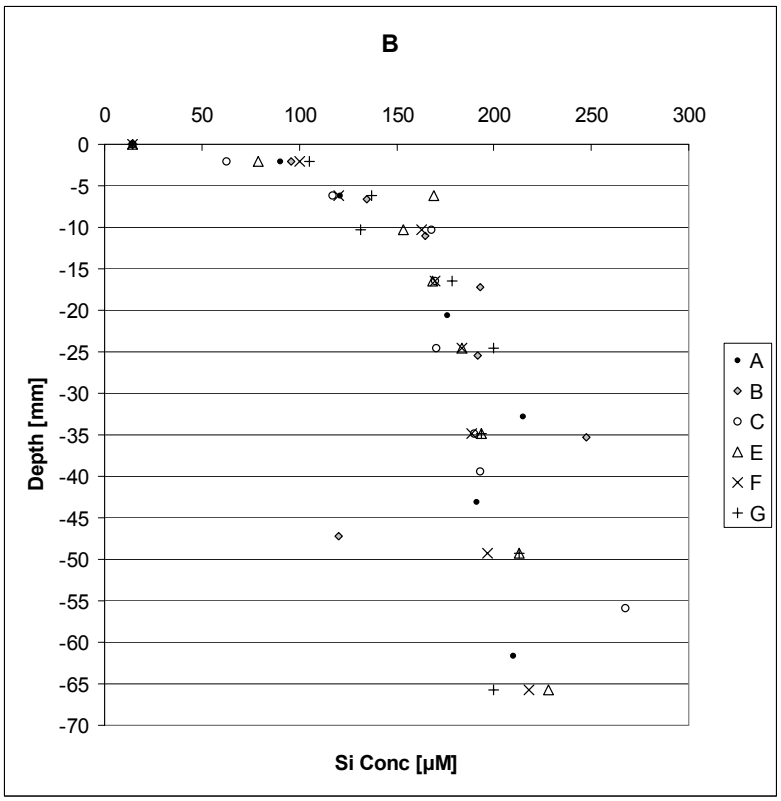
B
0
50
100
150
200
250
300
0
-5
-10
-15
-20
-25
-30
-35
-40
-45
-50
-55
-60
-65
-70
Depth [mm]
Si Conc [µM]
A
B
C
E
F
G

Fig 9

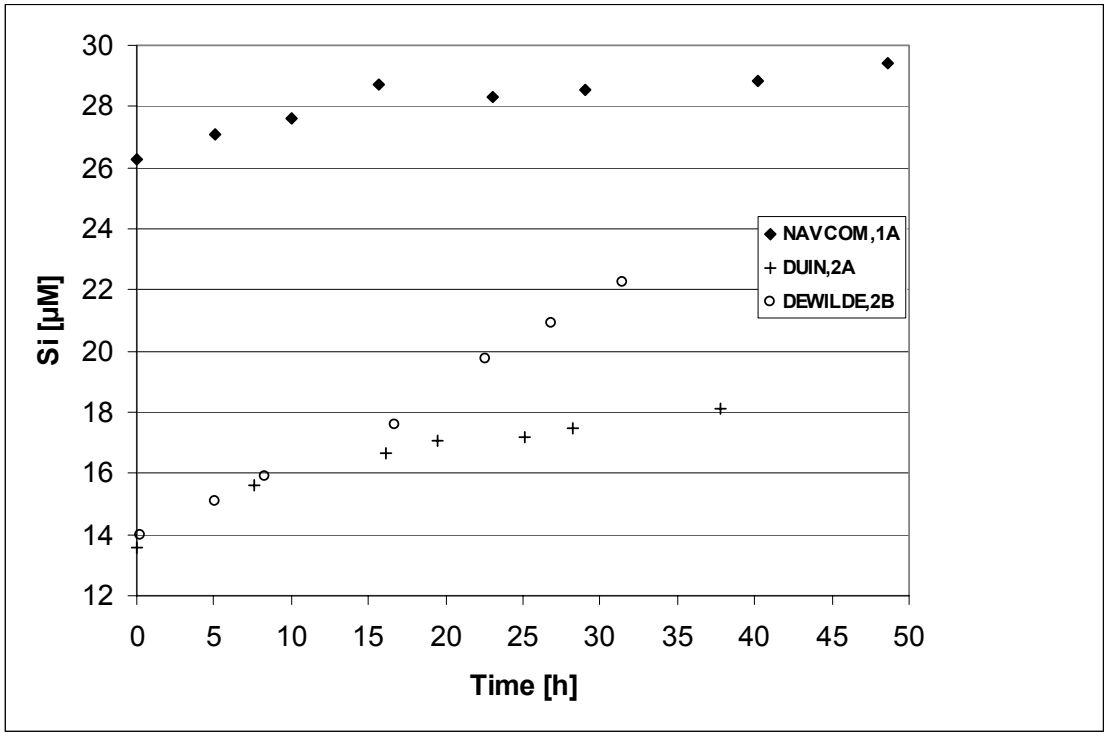
30
28
26
24
22
20
18
16
14
12
Si [µM]
0
5
10
15
20
25
30
35
40
45
50
Time [h]
NAVCOM,1A
DUIN,2A
DEWILDE,2B

Fig 10

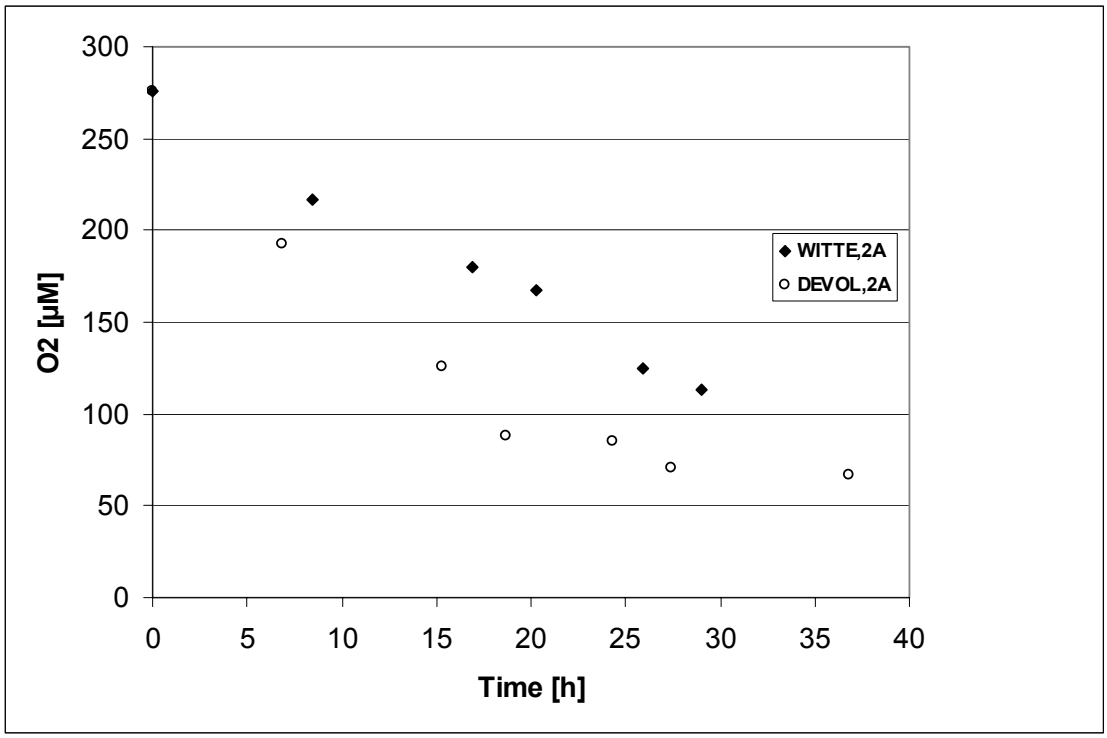
300
250
200
150
100
50
0
O2 [µM]
0
5
10
15
20
25
30
35
40
Time [h]
WITTE,2A
DEVOL,2A

Fig 11

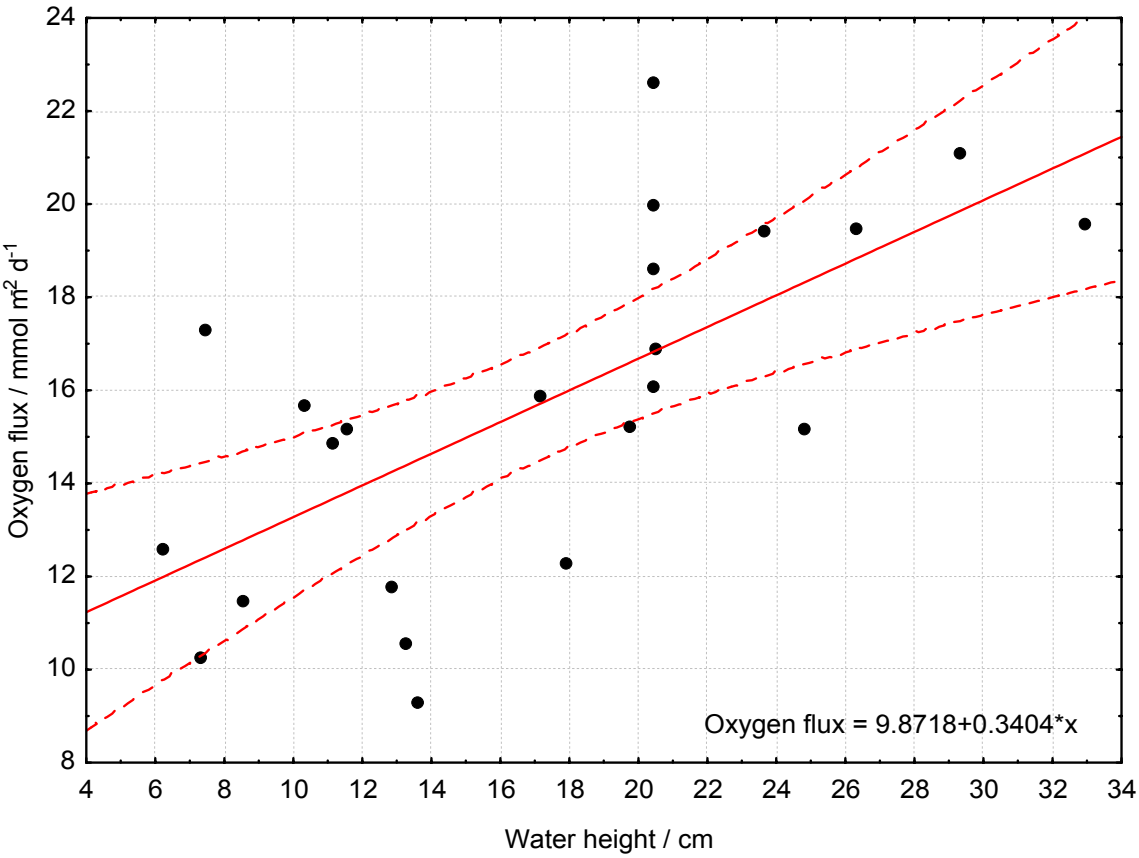
Oxygen flux / mmol m-2 d-1
Water height / cm
Oxygen flux = 9.8718+0.3404*x
24
22
20
18
16
14
12
10
8
4
6
8
10
12
14
16
18
20
22
24
26
28
30
32
34